Arctic decadal variability from an idealized atmosphere-ice-ocean model:
1. Model description, calibration, and validation

Dmitry Dukhovskoy,[1] Mark Johnson,[2] and Andrey Proshutinsky[3]

[1] This paper describes a simple "multibox" model of the Arctic atmosphere-ice-ocean system. The model consists of two major modules (an Arctic module and a Greenland Sea module) and several sub-modules. The Arctic module includes a shelf box model coupled with a thermodynamic sea ice model, and an Arctic Ocean model coupled with a sea ice model and an atmospheric box model. The Greenland Sea module includes an oceanic model coupled with a sea ice model and a statistical model of surface air temperature over the Greenland Sea. The full model is forced by daily solar radiation, wind stress, river runoff, and Pacific Water inflow through Bering Strait. For validation purposes, results from model experiments reproducing seasonal variability of the major system parameters are analyzed and compared with observations and other models. The model reproduces the seasonal variability of the Arctic system reasonably well and is used to investigate decadal Arctic climate variability in part 2 of this publication (Dukhovskoy et al., 2006).

Citation: Dukhovskoy, D., M. Johnson, and A. Proshutinsky (2006), Arctic decadal variability from an idealized atmosphere-ice-ocean model: 1. Model description, calibration, and validation, *J. Geophys. Res.*, *111*, C06028, doi:10.1029/2004JC002821.

1. Introduction

1.1. Problem Formulation

[2] Summarizing results from different studies of Arctic climate variability, *Proshutinsky et al.* [2002] formulated a conceptual model where freshwater and heat fluxes between the Arctic Ocean and GIN Sea play a crucial role in generating self-oscillating climate regimes with a period of 10–15 years. There are several ways to test this hypothesis. One of the most convincing approaches may be to analyze observations, but there are not enough data, and analysis of observational data would not allow us to investigate the mechanisms and roles of different factors that influence system behavior. Another approach is numerical modeling and using results from model runs. Climate models of different complexity (from very simple box models to extremely complex coupled global climate models) could be employed [*North*, 1975; *Saltzman*, 1985; *Henderson-Sellers and McGuffie*, 1987; *Häkkinen*, 2000; *Curry and Lynch*, 2002]. State-of-the-art coupled general circulation models of the atmosphere and the ocean have been developed and used to study decadal variability of Arctic climate, and its interaction with the North Atlantic Ocean, as well as the interaction between sea ice and global thermohaline circulation [*Manabe and Stouffer*, 1996; *Gordon and O'Farrell*, 1997; *Flato et al.*, 2000; *Gordon et al.*, 2000]. These types are considered to be "the most complete type of climate models currently available" [*Henderson-Sellers and McGuffie*, 1987]. However, in terms of delicate balances between the Arctic climate components and their poorly documented sensitivities, it is not surprising that climate models have not succeeded in explaining the observed changes in the Arctic climate system. Comparison with observations shows that "models have difficulty reproducing both the trends and the mean state of the Arctic, raising doubt over their ability to elucidate causative connections or predict future trends" [*Shindell*, 2003]. *Claussen et al.* [2002] warns against overestimating the reliability of the "state-of-the-art" models and argues that the description of the climate system should rely on a spectrum of climate system models, including simple conceptual models.

[3] The advantage of idealized climate models is their relatively simple formulation where only the major forces are included. Simple climate models have low computational cost and are designed to investigate the basic relationships between components of the climate system, the factors driving climate change and the overall response of the system [*Claussen et al.*, 2002].

[4] There are also models of intermediate complexity that still have enough simplicity to be used to understand the role of different forcing factors. Applications of this type of model for studies of Arctic climate variability [e.g., *Goosse et al.*, 2003; *Mysak et al.*, 2005] have shown promising results. Nevertheless, it is still difficult to determine where and how internal mechanisms work in the coupled atmosphere-ice-ocean system, so model output needs to undergo

---

[1]Center for Ocean-Atmospheric Prediction Studies, Florida State University, Tallahassee, Florida, USA.
[2]Institute of Marine Science, University of Alaska Fairbanks, Fairbanks, Alaska, USA.
[3]Physical Oceanography Department, Woods Hole Oceanographic Institution, Woods Hole, Massachusetts, USA.

complex data analysis to reduce uncertainty and find the major relationships and causes of climate variability.

[5] A simple model reproducing the major links and interactions among components of the Arctic climate system similar to *Proshutinsky et al.* [2002] must be able to simulate the mechanisms of decadal variability. Obviously such a model should include several simple, coupled models describing the essential processes. This could be done by employing an existing "multibox" climate model, however, one disadvantage of such models (discussed in the next section) is that, being constructed to solve a particular problem, they may be inadequate for our purposes. To meet our needs, we develop, validate, and calibrate a simple model of an idealized atmosphere-ice-ocean climate system.

1.2. Overview of Simple Models of the Arctic

[6] Relatively small horizontal gradients of temperature and salinity within the real Arctic Ocean enabled researchers to apply simple one-dimensional and box models to generate a realistic first-order description of the stratification and evolution of the upper Arctic Ocean [*Stigebrandt*, 1981; *Killworth and Smith*, 1984; *Lemke and Manley*, 1984; *Björk*, 1989]. For the Greenland-Iceland-Norwegian Seas (GIN Sea), simple models are mostly employed to simulate convection in the Greenland Sea [*Killworth*, 1979; *Houssais*, 1987; *Visbeck et al.*, 1995]. Table 1 lists a number of simple models of the Arctic climate study and their characteristics.

[7] The first simple dynamical models of the Arctic Ocean appeared in the early 1980s, and the simplest were characterized by few interacting components. Most of the simple models of the Arctic Ocean simulated processes in the upper ocean (above 200 m) [*Björk*, 1989; *Lemke and Manley*, 1984] and consisted of two layers: a homogeneous mixed layer and a pycnocline. Some models included the deep ocean [*Killworth and Smith*, 1984; *Alekseev and Ryabchenko*, 1996]. Deepening of the upper layer in the mixed layer models was based on Kato-Phillips [*Kato and Phillips*, 1969] and the Niiler and Kraus formulation [*Niiler and Kraus*, 1977] which parameterizes the rate of entrainment of fluid across the lower interface of the mixed layer, based on the balance of potential and kinetic energies in the layer.

[8] Entrainment depends on the density jump at the base of the mixed layer and the thermohaline structure of the underlying pycnocline. In some simple ocean models, the pycnocline was treated as a homogeneous layer [*Walin*, 1993; *Robitaille et al.*, 1995]. In other mixed layer models, the pycnocline structure was approximated by an analytical function, like the exponential function in *Lemke and Manley* [1984] or the parametric fitting of *Miropolsky et al.* [1969] used in *Alekseev and Ryabchenko* [1996]. In the model of *Björk* [1989], the thermohaline structure in the pycnocline was determined by vertical advection-diffusion equations for temperature and salinity.

[9] Following the classification of *Claussen et al.* [2002], the most advanced among simple models are simple "climate system models" which are applied to study long-term climate variability. The simple climate system models are constructed by coupling several box and one-dimensional models that simulate component processes in the climate

system. These models have more interacting components and a higher value of cumulative dimension.

[10] Several simple climate system models have been developed for the high latitude environment [e.g., *Robitaille et al.*, 1995; *Wang and Mysak*, 2000]. Among simple climate models of the Arctic Ocean – Greenland Sea region, the one by *Robitaille et al.* [1995] would seem appropriate for our problem. However, this model was not designed to reproduce oscillations. Also the formulation of the model contradicts our view of the problem: in *Robitaille et al.* [1995], the atmosphere completely controlled the system. In our mechanism the ocean affects the atmosphere through the heat fluxes from the GIN Sea. Also, the thermohaline structure of the Arctic Ocean cannot be resolved in a two-layer model such as Robitaille et al's.

[11] From the above it follows that in order to simulate our climate system there is no "ready-to-use" simple model. This caused us to develop our own simple model of the Arctic Ocean - Greenland Sea atmosphere-ice-ocean climate system. The description of the model components is presented in section 2. Validation of the model is given in section 3.

2. Model Description

[12] The Arctic system model consists of two modules: the Arctic module and the Greenland Sea module (Figure 1). The Arctic module includes a shelf box model coupled with a thermodynamic sea ice model and an Arctic Ocean model coupled with a sea ice model and an atmospheric box model.

[13] In the GIN Sea we focus on ocean overturning, air-sea flux, ice formation, and surface air temperature (SAT) anomalies in the convection region (Greenland Gyre). The Greenland Sea module includes an oceanic model of the central Greenland Sea region coupled with a sea ice model and a statistical model of SAT in the Greenland Sea. The module interaction between the Arctic Ocean and the Greenland Sea is realized through the freshwater flux (ice and water) from the Arctic Ocean, and atmospheric heat advection from the Greenland Sea. The ice-ocean components interact with the atmospheric models via the net surface heat flux.

[14] The model is forced by solar (shortwave downwelling) radiation, wind stress, river runoff, Atlantic inflow, Pacific Water inflow through Bering Strait, cloudiness, air humidity, and ice/snow albedo. The daily shortwave downwelling radiation values have been computed for 75°N and 85°N latitudes using equations of the Sun-Earth astronomical relationships [*Iqbal*, 1983]. Other forcing parameters have been prescribed with monthly means linearly interpolated into daily data [*Gorshkov*, 1980; *Lindsay*, 1998; *Polyakov et al.*, 1999]. The Notation section lists most notations used in the model.

2.1. Arctic Module: Arctic Ocean Model

[15] The Arctic Ocean model (Figure 2) describes seasonal and interannual variability in the upper ocean. The model is based on the pycnocline model of *Stigebrandt* [1985] modified and applied for the Arctic Ocean by *Björk* [1989]. In this study, the model has been further modified by new algorithms for: parameterization of forced convec-

Table 1. Simple Models of the Arctic and GIN Sea Region

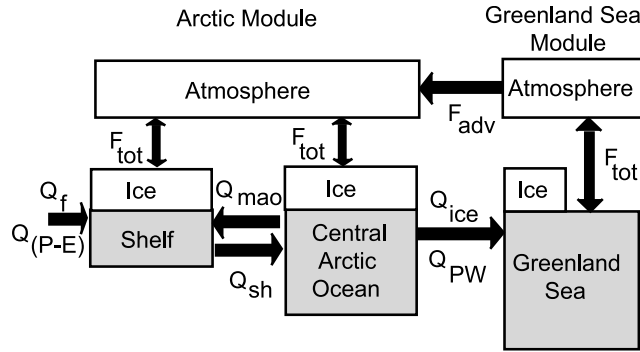| Year	Model	Simulated Regions	Research Goals	Forcing
1979	Quasi-static and time dependent models of vertical convection based on energy, salinity and temperature budgets of mixed layer and sea ice [Killworth, 1979]	Weddel Gyre, Greenland Sea Gyre	Study the development of chimney in the convection regions	Mixed layer thickness, ice production
1981	Two-layer (mixed layer and halocline) ocean box model [Stigebrandt, 1981]	Arctic Ocean	Study sensitivity of ice cover to the freshwater supply	Constant wind, water and ice transport at the lateral boundaries
1984	1-D halocline model [Killworth and Smith, 1984]	Arctic Ocean and shelf	Study vertical thermohaline structure	Constant river runoff, Bering Strait inflow, shelf water outflow, and Atlantic water inflow, surface salt flux
1984	1-D upper ocean model (mixed layer and halocline) [Lemke and Manley, 1984]	Arctic Ocean	Simulate seasonal variability of the upper Arctic Ocean	Monthly wind stress and surface salt fluxes
1987	1-D upper ocean (mixed layer and halocline) model coupled to a thermodynamic sea ice [Lemke, 1987]	Arctic Ocean, Southern Ocean	Study the effect of variations of the entrained oceanic heat flux on the sea ice cover	Monthly SAT and wind stress
1987	1-D ocean mixed layer model coupled to a thermodynamic sea ice model [Houssais, 1987]	Greenland Sea	Investigate the seasonal cycle of ice-ocean interaction in the subarctic ocean	Monthly surface heat fluxes, evaporation, precipitation, wind, and surface air temperature
1989	1-D pycnocline model (mixed layer and pycnocline) [Björk, 1989]	Interior Arctic Ocean and shelf	Simulate the upper ocean thermohaline structure	Monthly wind, river runoff, ice production and export, Bering Strait inflow
1990	1-D mixed layer model coupled to a three-layer snow-ice model [Häkkinen and Mellor, 1990]	Arctic Ocean	Simulate Arctic ice mass and mixed layer properties	Monthly wind, cloudiness, precipitation, SAT
1993	1-D 2 layer (homogeneous mixed and deep layers) ocean model coupled to an idealized ice model [Walin, 1993]	Greenland Sea	Study the development of deep convection in the ice covered ocean	Heat flux to the atmosphere, precipitation, oceanic heat flux to the ice,
1995	1-D model of the mixed layer with entrainment parameterized using critical Richardson numbers [Pawlowicz, 1995]	Greenland Sea Gyre	Study the evolution of the mixed layer in the convection region	SAT and wind
1995	Simple climate system model consisting of the upper ocean box model and thermodynamic ice model [Robitaille et al., 1995]	Arctic Ocean, Greenland Sea, Norwegian Sea, Greenland Sea Gyre	Study interaction between the Arctic and the GIN Sea and its effect on Arctic climate variability	Monthly mean SAT, river runoff, constant inflows at the lateral boundaries
1995	1-D mixed layer model coupled to a thermodynamic ice model [Visbeck et al., 1995]	Greenland Sea Gyre	Investigate evolution of the stratification in the Greenland Sea in winter	Constant heat, freshwater, wind stress fluxes at the ocean surface
1996	1-D 3-layer (upper mixed layer, the halocline layer, and the deep layer) ocean model coupled with a thermodynamic sea ice model [Alekseev and Ryabchenko, 1996]	Arctic Ocean	Study seasonal variability in the ocean-ice system	Monthly incoming shortwave radiation, surface air temperature, wind stress, cloudiness, air humidity, volume fluxes of the Bering Strait inflow, Atlantic water, and river runoff
1996	Multibox model of the upper Arctic Ocean coupled to an idealized ice model consisting of ridging and thermodynamics (look-up Tables) and advection [Steele et al., 1996]	Arctic Ocean	Examine the freshwater balance of the Arctic Ocean	Seasonally varying inflows at Bering Strait and constant inflow from the Kara Sea, monthly river runoff, net precipitation, constant wind stress
1999	1-D pycnocline model coupled to a model of ice volume [Rudels et al., 1999]	Weddell Sea, Greenland Sea	Study the relation between evolution of ice cover, heat loss to the atmosphere and ice melt, entrained heat and development of deep convection	Constant air humidity, air temperature, wind speed
1999	Simple climate system model consisting of coupled Manabe's bucket atmospheric model, zonally averaged global ocean, zero-layer thermodynamic sea ice model, and land model predicting surface temperature based on energy budget equations [Wang and Mysak, 2000]	North Atlantic Ocean	Long-term climate change studies	Solar radiation, zonally averaged monthly mean SST, wind stress

Figure 1. Diagram of an idealized Arctic system model. Q_f – river runoff; $Q_{(P-E)}$ – net precipitation (precipitation minus evaporation); Q_{mao} – flow from the mixed layer to the shelf; Q_{sh} – shelf water flow to the Arctic Ocean; Q_{ice} – ice flux to the GIN Sea; Q_{PW} – Polar water flux; F_{adv} – sensible heat flux; F_{tot} – surface heat flux.

tion dissipation; coupling with a thermodynamic sea ice model; inclusion of a shelf sub-model coupled with a thermodynamic sea ice model; a more complex mechanism of interaction between the Arctic Ocean and Arctic shelf; and rerouting river runoff from the Arctic basin to the shelf sub-model box.

[16] The Arctic Ocean model is one dimensional. It consists of three interacting layers (Figure 2): a surface mixed layer, an intermediate halocline layer with depth dependant temperature and salinity, and a deep Atlantic layer.

2.1.1. Mixed Layer

[17] The mixed layer is characterized by three parameters, thickness (h_{ml}), temperature (T_{ml}, assumed to be always at the salinity dependent freezing point) and salinity (S_{ml}). The surface mixed layer thickness depends on the ocean's vertical mixing rate (entrainment) and rates of change of the mixed layer depth due to changes in water fluxes into and out of the layer from different sources:

$$\frac{dh_{ml}}{dt} = \frac{1}{A_{AO}} \left(Q_{sh\_ml} - Q_{mao} + Q_{gML\_atl} + \mu_{Ber} \cdot Q_{Ber} + \varepsilon \cdot Q_{ice} \right) - w_e, \tag{1}$$

where A_{AO} is area of the deep Arctic Ocean (0.61×10^{13} m^2). Q_{sh_ml} is the fraction of the total shelf outflow (Q_{sh}) that inflows to the mixed layer. The rest of the outflow contributes highly-saline and cold water to the Arctic halocline (explained in section 2.2). The import of shelf water to the interior Arctic Ocean equals the prescribed outflow from the mixed layer on the shelf (Q_{mao}). Q_{gML_atl} is water volume flux from the mixed layer to the North Atlantic. The Pacific Water inflow through Bering Strait (hereinafter referred to as Bering Water, Q_{Ber}) has seasonally varying salinity (S_{Ber}) and temperature (T_{Ber}). The Bering Water is isopycnally mixed with the Arctic Ocean water flowing either to the mixed layer or halocline depending on the mixed layer density: $\mu_{Ber} = \begin{cases} 1, & \rho_{Ber} \leq \rho_{ml} \\ 0, & \rho_{Ber} > \rho_{ml} \end{cases}$, where ρ_{Ber} is density of

the Bering Water, ρ_{ml} is density of the mixed layer. The Arctic Ocean exports ice (Q_{ice}) to the North Atlantic through Fram Strait and channels of the Canadian Archipelago. $\varepsilon = \rho_{ice}/\rho_w \approx 0.9$, where ρ_{ice} is density of the sea ice, and ρ_w is density of sea water. w_e is the entrainment velocity.

[18] Similar to *Björk* [1989] and *Stigebrandt* [1981], the outflow Q_{g_atl} is assumed to occur as geostrophically balanced coastal currents with the underlying Atlantic water at rest. The outflow is estimated by integrating the thermal wind equation across the flow. There are two major outlets for the Arctic Ocean water: Fram Strait and channels of the Canadian Archipelago. The total number of geostrophic outlets (λ_{out}) is 1.5 assuming one full geostrophic outlet in the Fram Strait and half in the Canadian Archipelago (see *Björk* [1989] for more discussion on this parameter).

[19] According to *Björk* [1989], if the Y-axis is along the coast and the X-axis is across the flow with the coast located at $x = 0$, then the transport per unit depth across the outflow region is:

$$q_{atl}(z) = \int_0^{x_a} v_g \, dx = -\frac{g}{\rho_{atl} f} \int_z^{H_h} (\rho_{atl} - \rho(z)) \, dz, \tag{2}$$

where v_g is the coast-parallel velocity of the geostrophic flow, x_a is an offshore distance where $\rho(x, z) = \rho_{atl}$, ρ_{atl} is Atlantic water density, and H_h is total thickness of the mixed layer and halocline.
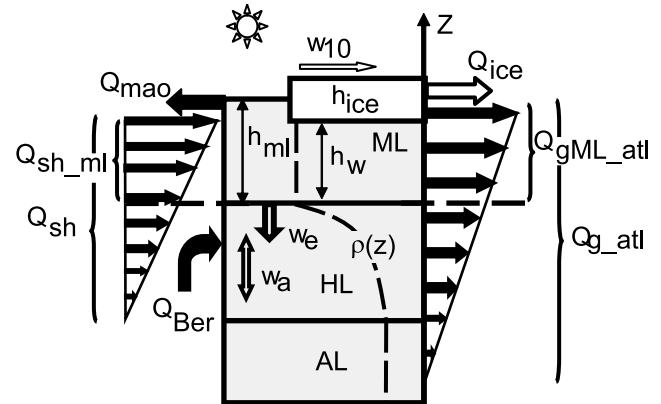

Figure 2. Diagram of the Arctic Ocean model. Three layers in the model: AL – Atlantic layer, HL – halocline layer, and ML – mixed layer. Q_{mao} is the outflow from the mixed layer to the shelf. Q_{sh} is the import of shelf water to the interior Arctic Ocean. Q_{sh_ml} is the fraction of Q_{sh} inflowing into the mixed layer. Q_{Ber} is the Bering Strait inflow with seasonally varying salinity (S_{Ber}) and temperature (T_{Ber}). Q_{ice} is the ice export from the Arctic Ocean and Q_{g_atl} is the water export from the Arctic Ocean to the North Atlantic through Fram Strait and channels of Canadian Archipelago. Q_{gML_atl} is the fraction of the Arctic Ocean water outflow from the mixed layer. h_{ml} is mixed layer thickness, h_w – mixed layer thickness measured from the base of the ice, w_{10} – wind, h_{ice} – ice thickness, w_e – entrainment velocity, w_a – vertical velocity, and $\rho(z)$ – water density.

[20] Water volume flux from the mixed layer to the North Atlantic is expressed as:

$$Q_{gML\_at} = \lambda_{out} \int_0^{h_{ml}} q_{atl}(z)dz, \tag{3}$$

and the total outflow from the mixed layer and halocline is:

$$Q_{g\_atl} = \lambda_{out} \int_0^{H_h} q_{atl}(z)dz. \tag{4}$$

The sign convention is $Q_{g\_atl} < 0$, meaning water export from the Arctic basin.

[21] The role of sea ice in the coupling of the Arctic Ocean and Greenland Sea is not our primary focus so the model is designed such that the long-term mean ice thickness is constant. All produced ice is exported from the Arctic model. The ice export (Q_{ice}) from the Arctic Ocean is a function of net gain or loss of ice in the Arctic relative to the previous year:

$$Q_{ice} = \bar{P}r_{i\_ao} \cdot A_{AO}, \tag{5}$$

where $\bar{P}r_{i\_ao}$ is the annual mean ice production from the previous year.

[22] The entrainment velocity is given by:

$$w_e = -\frac{1}{g'}\left[\frac{2m_0(u_*)^3}{h_w} - \kappa \cdot B_{fl}\right], \tag{6}$$

where g' is reduced gravity, h_w is the mixed layer depth measured from the base of the ice, m_0 and κ are proportionality coefficients which are discussed later. The friction velocity (u_*), is determined by wind from relations in *Thorndike and Colony* [1982], and the buoyancy flux at the sea surface (B_{fl}) is defined as:

$$B_{fl} = g\beta\left\{\frac{1}{A_{AO}}[Q_{sh\_ml}(S_{ml} - S_{sh\_ml}) + \mu_{Ber}Q_{Ber}(S_{ml} - S_{Ber})]\right.$$
$$\left. - \varepsilon Pr_{i\_ao}(S_{ml} - S_{ice})\right\}, \tag{7}$$

where g is gravitational acceleration, Pr_{i_ao} is ice production in the Arctic Ocean and β is the coefficient of salt contraction.

[23] When B_{fl} is positive (w_e may be negative or positive), the depth of the mixed layer is determined from Monin-Obukhov, Ekman length scales or equation (1) depending on values of B_{fl} and w_e. The detailed description of the length scales used for different dynamical regimes is given by *Stigebrandt* [1985]. In summary, when $B_{fl} > 0$ and $w_e > 0$ (retreat of the mixed layer) then the depth of the mixed layer is defined by the minimum value between h_{Ekm} and h_{Ob}: $h_{ml} = \min \{h_{Ob}, h_{Ekm}\}$, where h_{Ob} is the Monin-Obukhov length $\left(h_{Ob} = \frac{2m_0(u_*)^3}{B_{fl}}\right)$ and h_{Ekm} is the Ekman length

$\left(h_{Ekm} = \frac{K_e \cdot u^*}{f}\right)$. If $B_{fl} > 0$ and $w_e \leq 0$ (pure forced convection) then $h_{ml} = \min \{h_{ml}, h_{Ob}, h_{Ekm}\}$.

[24] Salinity changes in the mixed layer are computed from:

$$\frac{dS_{ml}}{dt} = \frac{1}{h_w}\left\{\frac{1}{A_{AO}}Q_{sh\_ml}(\bar{S}_{sh\_ml} - S_{ml}) + \varepsilon Pr_{i\_ao}(S_{ml} - S_{ice})\right.$$
$$\left. - w_e[S(h_{ml+}) - S_{ml}]\right\}, \tag{8}$$

where Q_{sh_ml} is the output (volume transport) from the shelf box model (discussed in the shelf model section), $\bar{S}_{sh\_ml}$ is the integrated salinity of the shelf outflow into the mixed layer (discussed later), and $S(h_{ml+})$ is salinity just below the mixed layer.

[25] The proportionality coefficient, m_0, that parameterizes dissipation of forced convection in equation (6) is:

$$m_0 = \log\left[\left(\frac{100}{Ri_o}\right)^P\right] + 3.5, \tag{9}$$

$$m_0 = \begin{cases} \max(0, m_0) \\ \min(8, m_0) \end{cases}, \tag{10}$$

where $Ri_o = \frac{h_{ml} \cdot g'}{u_*^2}$ is bulk Richardson number. Plausible mixed layer dynamics are obtained with P ranging from 1.2 to 2.0. In the model experiments $P = 1.2$ for the Arctic Ocean model and $P = 1.8$ for the Greenland Sea model.

[26] The mixed layer deepening rate driven by thermohaline convection is determined by the proportionality factor κ. The κ coefficient parameterizes dissipation of the convectively produced turbulence in equation (6). κ is a function of the water column stability: when stability is high the dissipation of convection is high as well. For the Arctic Ocean, which is characterized by year-round strong stratification, the κ coefficient is set to be 0.05 in agreement with *Björk* [1989].

2.1.2. Halocline Layer

[27] The halocline layer water temperature (T) and salinity (S) are calculated from:

$$\frac{\partial S}{\partial t} = w_a\frac{\partial S}{\partial z} + D_z\frac{\partial^2 S}{\partial z^2} + \frac{q_{sh}}{A_{AO}}(S(sh) - S(z)) + \mu_{Ber}\frac{Q_{Ber}}{A_{AO}}$$
$$\cdot (S_{Ber} - S(z)),$$

$$\frac{\partial T}{\partial t} = w_a\frac{\partial T}{\partial z} + D_z\frac{\partial^2 T}{\partial z^2} + \frac{q_{sh}}{A_{AO}}(T(sh) - T(z)) + \mu_{Ber}\frac{Q_{Ber}}{A_{AO}}$$
$$\cdot (T_{Ber} - T(z)). \tag{11}$$

where w_a is the vertical velocity, D_z is the coefficient of eddy diffusivity, $S(sh)$ and $T(sh)$ are salinity and temperature of the shelf outflow at a given vertical grid point where densities of the shelf water and halocline layer are the same (computing q_{sh} is presented in the shelf model section). The semi-implicit Crank-Nickolson scheme with Thomas algorithm [*Fletcher*, 1988] has been applied to get a numerical solution of equation (11). The vertical resolution (h_z) in the model is 1 m.
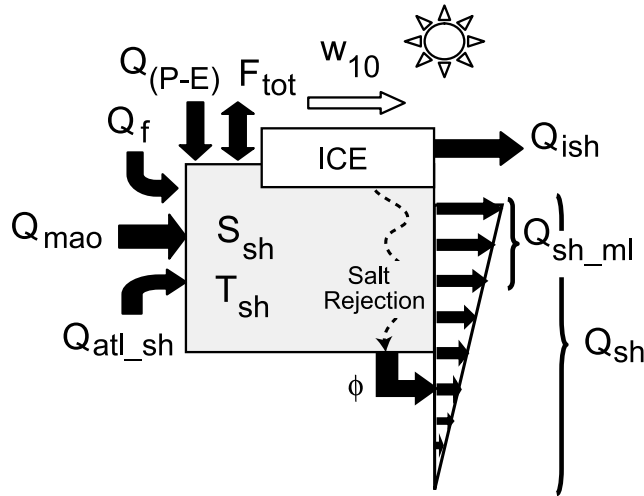
Figure 3. Diagram of the shelf box model. S_{sh} – shelf water salinity; T_{sh} – shelf water temperature, under ice-free conditions it is a function of surface heat flux (F_{tot}); ϕ - salt flux to the interior Arctic Ocean; w_{10} – wind; Q_f – river runoff; Q_{mao} – inflow from the Arctic Ocean mixed layer; Q_{atl_sh} – Atlantic water inflow to the shelf; $Q_{(P-E)}$ – net precipitation; Q_{ish} – ice export from shelf; and Q_{sh} – shelf flux to the Arctic Ocean. Upper part of the shelf flux (Q_{sh_ml}) goes to the Arctic Ocean mixed layer.

[28] The vertical velocity is calculated from the conservation of volume:

$$
w_a(z) = \begin{cases} -\dfrac{1}{A_{AO}} \cdot \left\{ \lambda_{out} \displaystyle\int_0^z q_{atl}(z)dz + \displaystyle\int_{S_{sh}}^{S_{sh\_out}(z)} q_{sh}(S)dS - Q_{mao} + \varepsilon \cdot Q_{ice} \right\}, & z \le z_{Ber} \\[6mm] -\dfrac{1}{A_{AO}} \cdot \left\{ \lambda_{out} \displaystyle\int_0^z q_{atl}(z)dz + \displaystyle\int_{S_{sh}}^{S_{sh\_out}(z)} q_{sh}(S)dS - Q_{mao} + \varepsilon \cdot Q_{ice} + Q_{Ber} \right\}, & z > z_{Ber}, . \end{cases}
$$

$$(12)$$

where $q_{sh}(S)$ is the shelf water outflow. This term, S_{sh} and S_{sh_out} are explained in section 2.2. z_{Ber} is the depth level of the Bering Water injection.

2.1.3. Atlantic Layer

[29] The Atlantic layer has constant temperature (T_{atl} = 0.5°C) and salinity (S_{atl} = 34.8).

2.2. Arctic Module: Shelf Box Model

[30] The Arctic shelf model is included in order to better reproduce fresh water and salt fluxes into the Arctic module. The area of the shelf region excluding the Barents Sea (A_{sh}) is 0.41 × 10^{13} m^2. A diagram of the shelf box model is shown in Figure 3. The shelf is represented with a box 50 m deep (h_{sh}) that exchanges water with the interior Arctic basin. There are four prescribed inflows: mixed layer water (Q_{mao}), river runoff (Q_f), Atlantic water brought onto the shelf through upwelling and advection from the Barents Sea (Q_{atl_sh}), and net precipitation ($Q_{(P-E)}$) which is precipitation minus evaporation. Arctic mixed layer water enters the box and is transformed by ice production or ice melting and

freshwater inflow. The outflowing water is interleaved in the interior Arctic Ocean at the isopycnal levels.

[31] The total volume outflow from the shelf to the interior basin (Q_{sh}) is equal to Q_{mao}. Q_{sh} is parameterized by means of an outflow function (Figure 4), $q_{sh}(S)$, which is a function of salinity:

$$ Q_{Sh} = \int_{Ssh}^{Sxx} q_{sh}(S)dS. \qquad (13) $$

The outflow from the shelf box is baroclinic and is constructed such that the intensity of the shelf outflow decreases as its salinity increases with depth (Figure 4a). The largest outflow (q_0) corresponds to S_{sh} and then decreases towards higher salinities, becoming zero at some threshold value S_{xx}. The area under the $q_{sh}(S)$ line equals the total shelf outflow Q_{sh}. It is obvious that S_{xx} depends on the ice production rate on the shelf. The less ice produced on the shelf, the less saline is the water flowing to the halocline. Thus S_{xx} is moving along the S (salinity) axis reaching S_{max} under the highest ice production rate (Figure 4a). When ice production is negative (Figure 4b) S_{xx} is approaching S_{sh} and $q_{sh}(S)$ becomes a Dirac delta function:

$$ \begin{cases} q_{sh}(S) = 0, & S \ne S_{sh} \\ \int q_{sh}(S)dS = q_{sh}(S_{sh}) = q_0 = Q_{sh}, & S = S_{sh} \end{cases}. \qquad (14) $$

[32] An important characteristic of the shelf-interior Arctic basin interaction in the model is the total outflow of salt (ϕ):

$$ \phi = \int_{Ssh}^{Sxx} q_{sh}(S) \cdot S \ \ dS. \qquad (15) $$

Also, it can be shown that ϕ is a function of ice production:

$$ \phi = (1 - \xi) \cdot \varepsilon \cdot Q_{ice}(S_{sh} - S_{ice}) + Q_{sh}S_{sh}, \qquad (16) $$

where ξ is a fraction of the rejected salt consumed to increase the shelf water salinity, namely, this amount of salt remains on the shelf: $\xi = \begin{cases} 0.2, & if \quad Pr_{i\_sh} > 0 \\ 1, & if \quad Pr_{i\_sh} \le 0, \end{cases}$ and Pr_{i_sh} is ice production on the shelf.

[33] Parameter S_{xx} determines the flow to the mixed layer and halocline of the Arctic Ocean model. In *Björk* [1989], S_{xx} is prescribed and constant (no seasonal variation), and

ice production on the shelf is obtained from the salt balance. In the presented model, the opposite approach is used: ice production is calculated in the thermodynamic sea ice model, which reproduces both seasonal and interannual signals, and S_{xx} is determined from the ice production. The following relationship between the ice production expressed in terms of ϕ, total shelf outflow Q_{sh} (which equals the prescribed Q_{mao}) and S_{xx} has been derived:

$$Q_{sh} = \frac{\phi(S_{xx} - S_{sh})^2}{S_{xx}(S_{xx}^2 - S_{sh}^2) - \frac{2}{3}(S_{xx}^3 - S_{sh}^3)} \tag{17}$$

The unknown S_{xx} is obtained by using the Newton-Raphson iteration technique [*Kreyszig*, 1999].

[34] Water temperature in the shelf model (T_{sh}) is calculated from different equations depending on whether or not there is ice cover in the model. When there is no ice:

$$\frac{dT_{sh}}{dt} = \frac{1}{h_{sh}} \cdot \left\{ \frac{F_{tot}}{\rho_{sh} \cdot C_{wp}} + \frac{1}{A_{sh}} \cdot [Q_{mao} \cdot (T_{ml} - T_{sh}) + Q_f \right.$$
$$\left. \cdot (T_f - T_{sh}) + Q_{atl\_sh} \cdot (T_{atl} - T_{sh})] \right\}, \tag{18}$$

where F_{tot} is the surface heat flux (positive to the ocean), ρ_{sh} is the shelf water density, C_{wp} is the water specific heat, T_{atl} is temperature of the Atlantic water, and T_f is the river runoff temperature. When ice appears in the model ($h_{ice} > 0$), temperature of the shelf water changes according to:

$$\frac{dT_{sh}}{dt} = \frac{1}{h_{sh}} \left\{ \frac{F_w}{\rho_{sh} \cdot C_{wp}} + \frac{1}{A_{sh}} \cdot [Q_{mao} \cdot (T_{ml} - T_{sh}) + Q_f \right.$$
$$\left. \cdot (T_f - T_{sh}) + Q_{atl\_sh} \cdot (T_{atl} - T_{sh})] \right\}, \tag{19}$$

where $F_w < 0$ is the water heat flux to the ice bottom.

[35] Salinity changes in the shelf model are described by the equation:

$$\frac{dS_{sh}}{dt} = \frac{1}{h_{shw}} \cdot \left\{ \frac{1}{A_{sh}} [Q_{mao}(S_{ml} - S_{sh}) - Q_f \cdot S_{sh} - Q_{(P-E)} \cdot S_{sh}] \right.$$
$$\left. + \xi \cdot \varepsilon \cdot Pr_{i\_sh}(S_{sh} - S_{ice}) \right\}, \tag{20}$$

where h_{shw} is depth of the shelf box measured from the base of the ice. When there is no ice in the box, $h_{shw} = h_{sh}$.

[36] The upper part of the shelf water outflow enters the mixed layer (Q_{sh_ml}) (Figures 2 and 3). Q_{sh_ml} is determined so that the density of the shelf water flowing into the mixed layer is less than or equal to the mixed layer density (ρ_{ml}). In summer, when no salt water is produced on the shelf and $S_{xx} < S_{ml}$, all shelf water flows into the mixed layer ($Q_{sh\_ml} = Q_{sh}$). During the cold season when salt is rejected from ice, the fraction of Q_{sh} with density higher than ρ_{ml} flows into the halocline. In this model, such events occur when $S_{xx} > S_{ml}$ (Figure 4). It is assumed that saline shelf water isopycnally mixes with the halocline water. The outflow function $q_{sh}(S)$ is a function of salinity. Hence, in order to determine the shelf water outflow into the halocline of the Arctic Ocean at a given depth z, the corresponding salinity of the shelf outflow at this depth level ($S_{sh\_out}(z)$) has to be
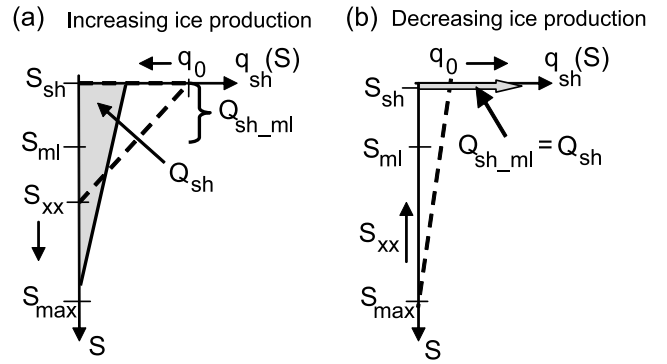

Figure 4. The outflow function. The largest outflow (q_0) corresponds to S_{sh} and then decreases towards higher salinities, becoming zero at salinity $S = S_{xx}$. The area under the $q_{sh}(S)$ line equals the total shelf outflow Q_{sh}. When ice production is high and positive (a), S_{xx} increases and q_0 decreases. When ice production weakens (b), S_{xx} decreases and q_0 grows. When ice production becomes negative (ice melt), $q_0 = Q_{sh}$. In case of negative ice production, $q_{sh}(S)$ is a Dirac delta function.

determined. To find $S_{sh\_out}(z)$ below the mixed layer, the initial condition is

$$\rho_{ao}(z) = \rho_{sh\_out} \left\{ T_{fr}[S_{sh\_out}(z)], S_{sh\_out}(z) \right\} \tag{21}$$

where ρ_{ao} is the Arctic Ocean density at a given depth level (z), ρ_{sh_out} is the density of the shelf outflow, $T_{fr}[S_{sh\_out}(z)]$ is the freezing temperature for given salinity of the shelf outflow ($S_{sh\_out}(z)$) (the water temperature of plumes is at the freezing point). Given ρ_{ao}, $S_{sh\_out}(z)$ is obtained from equation (21) by an iteration. Finally, $q_{sh}[S = S_{sh\_out}(z)]$ is calculated:

$$q_{sh}(S) = \frac{q_0(S_{xx} - S)}{S_{xx} - S_{sh}}. \tag{22}$$

2.3. Arctic Module: Sea Ice Model

[37] In order to simulate sea-ice, the Arctic Ocean and the shelf models are coupled to a thermodynamic linear sea ice model [*Maykut and Untersteiner*, 1969; *Maykut*, 1986]. The ice model computes sea ice growth and melting rates. All fluxes at the ice/snow – atmosphere and ocean-ice boundaries are calculated from the equations given in *Maykut and Untersteiner* [1969], *Maykut* [1986], and *Makshtas* [1991]. Accumulation of snow on the ice surface is parameterized by a linear time-dependent function of given ice thickness [*Doronin*, 1997]. The maximum snow thickness in the Arctic Ocean model is limited to 0.4 m, and to 0.3 m in the shelf and Greenland Sea models. Constants used in computations of the ice-atmosphere heat fluxes are given in Table 2.

2.4. Arctic Module: Atmospheric Model

[38] A conceptual energy balance box model for the Arctic atmosphere is presented in Figure 5. The surface air temperature ($T_{(0)}$) is calculated from the following:

$$\frac{dT_{(0)}}{dt} = \frac{F_{tot\_a}}{H_{atm}\rho_{air}C_p}, \tag{23}$$

Table 2. Constants in the Sea Ice Model

Constant	Value	Units
Penetration of the shortwave radiation in the ice (i_0)	0.3	
Longwave emissivity of the ice (ε_L)	0.97–0.99	
Stefan-Boltzman constant (σ)	5.67×10^{-8}	W m^{-2} °K^{-4}
Air specific heat (C_p)	1012	J kg^{-1} °K^{-1}
Air density (ρ_{air})	1.37	kg m^{-3}
Bulk transfer coefficient for sensible heat (C_s)	1.5×10^{-3}	
Latent heat of vaporization (L_{vp})	2.55×10^6	J·kg^{-1}
Bulk transfer coefficient for latent heat (C_e)	0.55×10^{-3}	
Constants for Calculating the Saturation Vapor Pressure		
E_0	611	Pa
a_1 (ice)	9.5	
b_1 (ice)	265.5	
a_1 (water)	7.63	
b_1 (water)	241.9	
Thermal conductivity in snow (k_{snow})	0.31	W m^{-1}·°K^{-1}
Thermal conductivity in ice (k_{ice})	2.05	W m^{-1}·°K^{-1}
Thermal conductivity in pure ice (k_0)	2.03	W m^{-1}·°K^{-1}
Penetration of the shortwave radiation in ice (i_0)	0.3	

where $H_{atm} = 8 \times 10^3$ m is the height of the atmospheric box, $\rho_{air} = 1.37$ kg·m^{-3} is the air density, and $C_p = 1012$ J·kg^{-1}·K^{-1} is the air specific heat. The total energy gain or loss in the box (F_{tot_a}) is estimated through the energy balance:

$$F_{tot\_a} = F_{tot(0)} + F_{tot(1)} + F_{adv}, \qquad (24)$$

where $F_{tot(0)}$ is the energy balance at the bottom atmospheric box boundary (atmosphere – ice), $F_{tot(1)}$ is the energy balance at the upper atmospheric box boundary (atmosphere – space), and F_{adv} is sensible heat advected from the Greenland Sea box. The energy balance at the bottom boundary ($F_{tot(0)}$) is calculated in the ice model of the Arctic Ocean.

[39] The energy balance at the upper boundary ($F_{tot(1)}$) is computed from the equations in *Wallace and Hobbs* [1977]. The heat advection to the Arctic (F_{adv}) depends on the SAT gradient between the Greenland Sea and Arctic boxes. This idea is adopted from *Marotzke and Stone* [1995] and *Scott et al.* [1999], who investigated atmospheric meridional transports and ocean-atmosphere interactions. *Marotzke and Stone* [1995] used a simplified parameterization assuming that the transport is proportional to the meridional temperature gradient to describe the meridional atmospheric heat transport between "cold" and "warm" boxes in their model:

$$F_{adv} = \chi(T_2 - T_1), \qquad (25)$$

where χ is the coefficient of heat advection, T_2 and T_1 are SAT in the warm and cold boxes respectively. The physical meaning of χ is the following. Because transient eddies (traveling highs and lows) are responsible for most of the meridional atmospheric transports in high latitudes [*Marotzke and Stone*, 1995], the coefficient χ is used to regulate the intensity of meridional heat transport, allowing higher transport as the temperature gradient increases. This simple relation (equation (25)) captures the salient feature of *Stone and Yao*'s [1990] parameterization of meridional eddy heat and moisture fluxes: as the meridional temperature gradient increases eddy activity increases as well. *Marotzke*

and Stone [1995] analytically estimated this coefficient to be 1.3 W · m^{-2} ·°K^{-1}. It describes the heat diffusion into the "cold" box in their simplified ocean-atmosphere box model. In our model, the estimate of χ is obtained empirically from a number of model experiments (see section 4 for brief discussion).

2.5. Greenland Sea Module: Ocean Model

[40] The oceanic model describes the development of the thermohaline structure in the Greenland Gyre. The model consists of several layers shown in Figure 6. The appearance and growth of the ice depends on the heat budget of the sea surface and characteristics of the mixed layer.
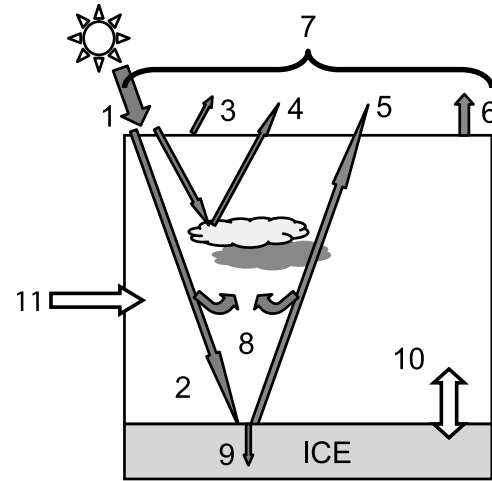

Figure 5. Diagram of the Arctic atmospheric box model. Numbers denote the fluxes: 1 – incoming solar radiation (F_{ins}); 2 - incoming on the ice shortwave radiation (F_{shw_inc}); 3 – back-scattered by air solar radiation (F_{rfl1}); 4 – reflected by clouds solar radiation (F_{rfl2}); 5 – reflected by ice surface (F_{rfl3}); 6 - longwave flux at the top of the atmosphere ($F_{lw(1)}$); 7 – energy balance at the upper boundary ($F_{tot(1)}$); 8 - absorbed shortwave radiation by the atmosphere (F_{atm_abs}); 9 - penetrated into ice shortwave radiation (F_{abs}); 10 - surface heat flux at the lower boundary ($F_{tot(0)}$); and 11 – meridional sensible heat transport from the Greenland Sea domain (F_{adv}).
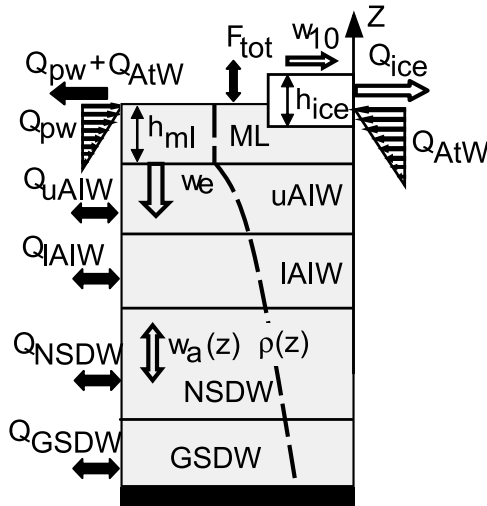
Figure 6. Greenland Sea Ocean Model. ML− mixed layer; uAIW − upper Atlantic Intermediate Water; lAIW − lower Atlantic Intermediate Water; NSDW − Norwegian Sea Deep Water; and GSDW − Greenland Sea Deep Water. F_{tot} − surface heat flux; w_e − entrainment velocity; w_a − vertical velocity; $\rho(z)$ − water density; h_{ice} − ice thickness; w_{10} − wind; and h_{ml} − mixed layer thickness. Volume fluxes: Q_{PW} − Polar Water; Q_{AtW} − Atlantic Water; Q_{ice} − ice export from the Greenland Sea; Q_{uAIW}, Q_{lAIW}, Q_{NSDW}, and Q_{GSDW} − inflow/outflow rates within the layers.

Evolution of the ice cover is simulated by the ice model and is identical to that in the Arctic Ocean module (section 2.3).

[41] The inflow in the Greenland Sea model is presented in Figure 6. To conserve mass, outflow from each layer equals the inflow. The Polar Water inflow (Q_{PW}) is a fraction of the Arctic Ocean outflow Q_{g_atl} integrated from the surface to 150 m depth. The temperature (T_{PW}) and salinity (S_{PW}) of Q_{PW} are integrated values of Q_{g_atl} within the same depth range.

[42] It should be noted that there is not enough observational data to explain how surface water is formed in the central Greenland Sea. It is generally believed that the Greenland Gyre experiences a very small effect from the East Greenland Current (EGC), receiving very little of the Polar Water [*Swift*, 1986; *Aagaard and Carmack*, 1989, 1994; *Alekseev et al.*, 1994]. Also it is assumed that the inflow rates of the Polar Water and Atlantic Water have seasonal variability. In winter, when the cyclonic vortex in the Greenland Gyre is intensified, the surface water is forced away from the Gyre center and very little ambient water can penetrate the Arctic front [*Swift*, 1986]. However in summer, when cyclonic vorticity is significantly weakened, the ambient surface water and sea ice can easily penetrate the front and reach the center of the Gyre [*Johannessen*, 1986]. This idea is well corroborated by oceanographic observations [*Pawlowicz*, 1995] showing freshening of the central Greenland Sea in summer. During summer, the EGC advects ice into the Greenland Sea model where it melts (Q_{mlt_GS}).

[43] The central part of the upper Greenland Sea consists of modified, diluted and cooled Atlantic Water. This water mass (Arctic Surface Water) results from mixing PW and AtW and is modified by air-sea interaction. The PW is 150 m thick

(H_{PW}) and includes water from the Arctic Ocean mixed layer and halocline. Thickness of the AtW (H_{AtW}) flowing into the central Greenland Sea is also 150 m. Thickness of the PW and AtW jets is based on *Swift* [1986] and *Swift and Aagaard* [1981]. Assuming that most interaction between the PW and AtW occurs in the very upper part of the central Greenland Sea, the vertical structure of the flows is approximated with linear functions q_{AtW} and q_{PW}, respectively:

$$q_{AtW}(z) = \begin{cases} q_{0,AtW} - \dfrac{q_{0,AtW}}{H_{AtW}}|z|, & |z| \leq H_{AtW} \\ 0, & |z| > H_{AtW}, \end{cases} \quad (26)$$

$$q_{PW}(z) = \begin{cases} q_{0,PW} - \dfrac{q_{0,PW}}{H_{PW}}|z|, & |z| \leq H_{PW} \\ 0, & |z| > H_{PW}, \end{cases} \quad (27)$$

where q_0 is the transport at the surface.

[44] Parameterization of the Greenland Sea mixed layer dynamics is similar to that of the Arctic Ocean. The length scale h_{ml} in the Greenland Sea is defined as:

$$\frac{dh_{ml}}{dt} = w_e + w_a. \quad (28)$$

The entrainment velocity is given by equation (6) with κ parameterized by the water column stability and buoyancy flux.

[45] Greenland Sea model sensitivity runs have shown that $\kappa = 0.05$ is too low and underestimates the role of convection in the mixed layer deepening (see section 4). Deep mixing in the Greenland Gyre occurs in small-scale "chimneys" driven by intense wintertime convection. We assume that the mixed layer in the Greenland Gyre is deep when "chimney" convection occurs in the region. To permit "chimney" scale convection, the Richardson number is defined by [*Chapman*, 1997]:

$$Ri = g' h_{ml} \left(|B_{fl}| r_0\right)^{-2/3}, \quad (29)$$

where h_{ml} is the mixed layer depth, B_{fl} is the buoyancy flux through the surface, and r_0 is the radius of a convective region taken to be 50 km. According to *Chapman* [1997], if the Richardson number (Ri_o) is greater than the transition Richardson number (Ri_T) which equals 8, the density gain in the upper layer (due to negative buoyancy flux) cannot overcome the density jump between the upper and lower layers. In this case convection should not penetrate into the lower layer and convection is strongly suppressed leading to a very small κ. If $Ri < Ri_T$ then, according to *Chapman* [1997], convection penetrates into the lower layer very fast and is not depth limited, assuming large κ. From the above theoretical discussions and model experiments, the following expressions for κ have been obtained when $B_{fl} < 0$:

$$\kappa = \begin{cases} 0.9, & \text{if} \quad Ri_o < Ri_T \\ 0.01 \cdot \log\left(\frac{3000}{h_{ml}}\right), & \text{if} \quad Ri_o > Ri_T \end{cases}. \quad (30)$$

When $B_{fl} > 0$, $\kappa = 1$.

[46] The vertical velocity is estimated through the Ekman pumping – wind stress curl relation [*Cushman-Roisin*, 1994]:

$$w_a = \frac{1}{\rho_0 f}\left(\frac{\partial \tau_y}{\partial x} - \frac{\partial \tau_x}{\partial y}\right) = \frac{1}{\rho_0 f}curl(\tau_{x,y}). \quad (31)$$

The wind stress curl over the Greenland Sea is adopted from *Jonsson* [1991].

[47] The buoyancy flux to the mixed layer is calculated using the following equation [*Turner*, 1973; *Stigebrandt*, 1981, 1985]:

$$B_{fl} = g \cdot \left\{ \frac{\alpha}{\rho_{ml} \cdot C_{wp}}F_{tot} + \frac{\beta}{A_{GS}} \right.$$
$$\cdot \left[(S_{ml} - S_{AtW})\int_0^{h_{ml}} q_{AtW}dz + (S_{ml} - S_{PW})\int_0^{h_{ml}} q_{PW}dz \right]$$
$$\left. - \varepsilon \cdot \beta \cdot (S_{ml} - S_{ice})\left(Pr_{i\_GS} + \frac{Q_{mlt\_GS}}{A_{GS}}\right) \right\} \quad (32)$$

where α and β are the coefficients of heat expansion and salt contraction, respectively; ρ_{ml} is the mixed layer density calculated through the equation of state, $C_{wp} = 4184.4$ J m^{-2}·sec^{-1} is the water specific heat, F_{tot} is the air-sea heat flux (positive for the flux to the ocean), A_{GS} is the area of the central Greenland Sea, and Pr_{i_GS} is ice production in the region. Q_{mlt_GS} is the volume of ice advected from the EGC and melted in the central Greenland Sea during summer.

[48] The salinity changes in the mixed layer are described by the salt balance equation:

$$\frac{dS_{ml}}{dt} = \frac{1}{h_w} \cdot \left\{ \frac{1}{A_{GS}} \right.$$
$$\cdot \left[(S_{AtW} - S_{ml})\int_0^{h_{ml}} q_{AtW} \cdot dz + (S_{PW} - S_{ml})\int_0^{h_{ml}} q_{PW} \cdot dz \right]$$
$$+ \varepsilon(S_{ice} - S_{ml})\left(\frac{Q_{mlt\_GS}}{A_{GS}} - Pr_{i\_GS}\right) - w_e$$
$$\left. \cdot \frac{[S(h_{ml+}) - S_{ml}]}{h_z} \right\}, \quad (33)$$

where Pr_{i_GS} is the ice production/melting rate (if there is any ice) and $S(h_{ml+})$ denotes the salinity just below the mixed layer. Equation (33) is valid only for downward entrainment velocity ($w_e < 0$), otherwise (during the mixed layer retreat) there is no w_e term in the formula.

[49] Under ice free conditions the temperature changes are given by:

$$\frac{dT_{ml}}{dt} = \frac{1}{h_w} \cdot \left\{ \frac{F_{tot}}{\rho_w C_{wp}} + \frac{1}{A_{GS}} \right.$$
$$\cdot \left[(T_{AtW} - T_{ml})\int_0^{h_{ml}} q_{AtW} \cdot dz + (T_{PW} - T_{ml})\int_0^{h_{ml}} q_{PW} \cdot dz \right]$$
$$\left. - w_e \cdot \frac{[T(h_{ml+}) - T_{ml}]}{h_z} \right\} \quad (34)$$

where $T(h_{ml+})$ is the water temperature just below the mixed layer. When accretion begins, F_{tot} in equation (34) is replaced with the heat flux from the water to the ice bottom (F_w) parameterized by the relation from *Maykut and Untersteiner* [1969].

[50] Below the mixed layer the local rate of change of the salinity and the temperature are:

$$\frac{\partial S}{\partial t} = w_a\frac{\partial S}{\partial z} + D_z\frac{\partial^2 S}{\partial z^2} + \frac{q_{in}(z)}{A_{GS}}[S_{in} - S(z)]$$
$$\frac{\partial T}{\partial t} = w_a\frac{\partial T}{\partial z} + D_z\frac{\partial^2 T}{\partial z^2} + \frac{q_{in}(z)}{A_{GS}}[T_{in} - T(z)], \quad (35)$$

where q_{in} denotes an inflow of water with temperature T_{in} and salinity S_{in} at a given depth z.

2.6. Greenland Sea Module: Statistical Model of SAT

[51] In the suggested mechanism of decadal variability, the FW ocean perturbations from the Arctic to the GIN Sea influence the atmosphere through convection, heat flux, and the sea ice freeze/melt cycle. Surface heat flux anomalies induce SAT anomalies in the region [*Häkkinen and Cavalieri*, 1989; *Häkkinen*, 1995] and a regional relation between surface heat flux and SAT anomalies is sought. A multiple regression model [*Chatfield*, 1996] has been developed to predict the next-day SAT anomaly given the previous day's heat flux and SAT.

[52] A high-order multiple regression model with a backward elimination technique [*Jennrich*, 1995] has been applied to select the final model:

$$Y_t = \alpha_1 Y_{t-1} + \alpha_2 Y_{t-2} + \alpha_3 Y_{t-3} + \beta_1 X_{t-1} + \beta_2 X_{t-2} + \varepsilon, \quad (36)$$

where Y_{t-i} denotes SAT anomaly on the ith previous day, X_{t-i} is the total net flux anomaly on the ith previous day, α's and β's are parameters to be estimated, ε is an error which is, in the case of a good fit, an independent Gaussian random variable.

[53] The model given by equation (36) differs from usual simple linear regression models in that there are two explanatory variables (X and Y). The first part of the model containing Y's is a third-order auto-regressive model. The second part with X's describes auto-correlated structure of the residual. Both model selection and parameter estimates have been done using SAS – the statistical programming language. The SAS output for the final model (equation (36)) is given in Tables 3 and 4. The over-all fit test (F - test) proves a good fit. All t - tests reveal that the parameters are significantly different from zero at confidence level $\alpha = 0.05$ (except for intercept which is zero).

[54] To validate the SAT statistical model, a 1-day forecast of SAT in the central Greenland Sea has been run for 1990–2000 using the National Centers for Environmental Prediction (NCEP) reanalysis data. The statistical model gives very accurate 1-day prediction (Figure 7a). The histogram (Figure 7b) and autocorrelation function (Figure 7c) of the residual show that the error term (ε) is white noise with a standard normal distribution; this also supports the idea that the model

Table 3. Analysis of Variance and *F*-Test of the Overall Fit

Source	DF[a]	Sum of Squares[b]	Mean Square[c]	*F* value[d]	*P* value[e]
Corrected total[f]	4011	3648.04			
Error[g]	4006	1441.97	0.35995		
Model[h]	5	2206.07	441.21	1225.76	<0.0001

[a]Degrees of freedom, which is (number of observations – (number of parameters plus intercept)).

[b]Sum of squared errors; errors are the difference between the model and observations.

[c]Mean Square Error = Sum of Squares/DF.

[d]Test for the overall model fit, null hypothesis (H_0) is that all coefficients in the model are zero (except for the intercept); F = Mean Square Model/Mean Square Error.

[e]Probability that a random value from $F(5,4006)$ distribution will exceed the observed $F = 1225.76$. If P-value is less than the confidence level α, H_0 is rejected which proves that the model fits the data well.

[f]Restricted model with all coefficients (parameters) zero except for the intercept.

[g]Complete (tested) model (equation (36)).

[h]Statistic is calculated from columns [a] and [b] obtained by subtraction of row [g] from [f].

(equation (36)) provides reliable 1-day forecasts of SAT anomalies in the region.

3. Model Calibration and Validation Results

[55] Calibration and validation experiments and sensitivity studies were conducted for each module and for the entire model. The forcing parameters applied in the model run are presented in Figures 8–10.

3.1. Model Initialization

[56] The full model was run to validate the behavior of the simulated system, i.e. to estimate how accurately the model reproduces the annual cycle. During the model run, daily values of the oceanic (T, S, h_{ml}, w_e, B_{fl}), ice (h_{ice}, Pr_{i_AO}, Pr_{i_GS}, Pr_{i_sh}), and atmospheric (T_0) characteristics and fluxes between the sub-models were calculated and compared with observations or output from other modeling studies. For this experiment, the statistical model of the SAT in the Greenland Sea was not employed. Instead, the SAT was assigned the daily mean values calculated from the NCEP reanalysis (Figure 10).

[57] The model was initialized with multiyear mean ocean temperature and salinity data and atmospheric SAT for the central Arctic, the Eurasian shelf, and the Greenland Sea acquired from the *Environmental Working Group* (*EWG*) [1998] atlas, the NOAA-CIRES Climate Diagnos-

Table 4. Parameter Estimates and Individual *t*-Tests

Variable	Parameter Estimate[a]	Standard Error[b]	*t* Statistics[c]	*P* Value[d]
Intercept	-1.65×10^{-4}	0.00947	−0.02	0.9861
α_1	0.80465	0.02256	35.67	<0.0001
α_2	−0.10905	0.02617	−4.17	<0.0001
α_3	0.10229	0.01574	6.50	<0.0001
β_1	0.08298	0.01988	4.17	<0.0001
β_2	−0.12	0.01976	−6.07	<0.0001

[a]Estimates for the intercept, α's and β's in the model (equation (36)).

[b]STD of the estimates.

[c]Individual *t*-tests for testing the hypothesis $\alpha_1 = 0$, $\alpha_2 = 0$, $\alpha_3 = 0$, $\beta_1 = 0$, and $\beta_2 = 0$.

[d]*P*-value, the probabilities that the absolute value of the corresponding *t*-statistic will exceed that of the *t*-value given, under the standard normality assumptions and assuming that the true parameter is zero. When *P*-value is less than the confidence level $\alpha = 0.05$, the null hypothesis is rejected.
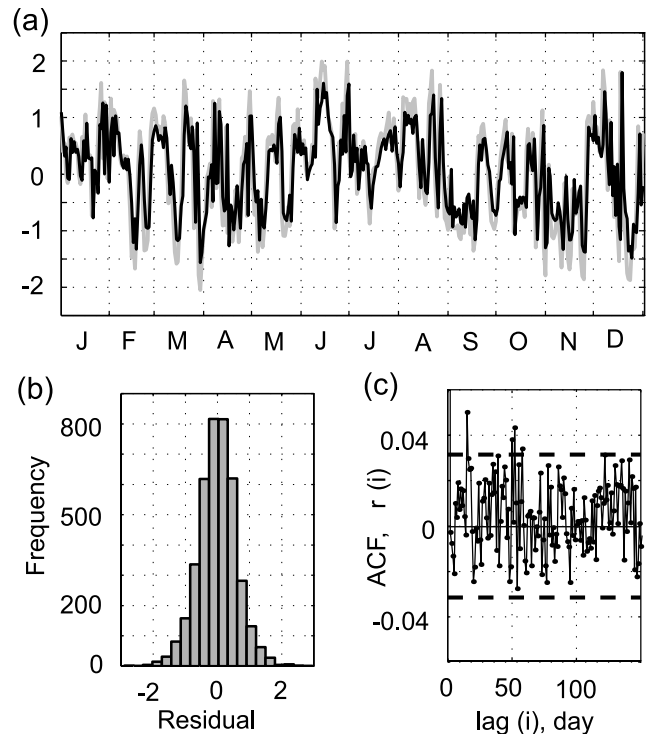

Figure 7. One day prediction from the statistical model of SAT anomalies for the central Greenland Sea for 1990–2000. (a) NCEP reanalysis SAT data (gray curve) and model predicted SAT (black curve) shown for 1991. (b) and (c) Analysis of the residual (1990–2000). The histogram (Figure 7b) and auto-correlation function (Figure 7c) of the residual (predictions minus observations) unambiguously prove that the error term (ε) is white noise with a standard normal distribution. Note scale of the vertical axis in Figure 7c; $r(i)$ is 1 at zero lag (not shown).

tics Center (CDC), and the Polar science center Hydrographic Climatology (PHC, http://psc.apl.washington.edu/POLES/PHC2) [*Steele et al.*, 2001]. The outflow from the Arctic Ocean to the Greenland Sea (Q_{g_atl}) was computed in the Arctic Ocean (equation (4)). The heat advection to the Arctic was obtained from equation (25) with the coefficient of heat advection (χ) set to 1.8 W · m^{-2} ·°K^{-1}. Water export from the Arctic Ocean mixed layer to the shelf (Q_{mao}) was taken to be 1.1 Sv.

3.2. Simulated and Observed Annual Cycles

[58] The model was run for 110 years. The simulated system reaches steady state after approximately 10 years. The results show that the mean annual cycle was reproduced in the sub-models for the Arctic, shelf, and Greenland Sea.

3.2.1. Arctic Ocean

[59] The calculated mixed layer thickness and salinity are presented in Figures 11a and 11b. The Arctic mixed layer is deepest in winter when it reaches 30–60 m and much shallower (up to 5–20 m) in summer [*Aagaard et al.*, 1981; *Stigebrandt*, 1981; *Swift et al.*, 1997]. The model reproduces a shallow mixed layer in summer (∼10 m) which deepens during the cold season and reaches the maximum thickness (∼27 m) in April–May (Figure 11a). Note the rapid shallowing of the mixed layer in the early
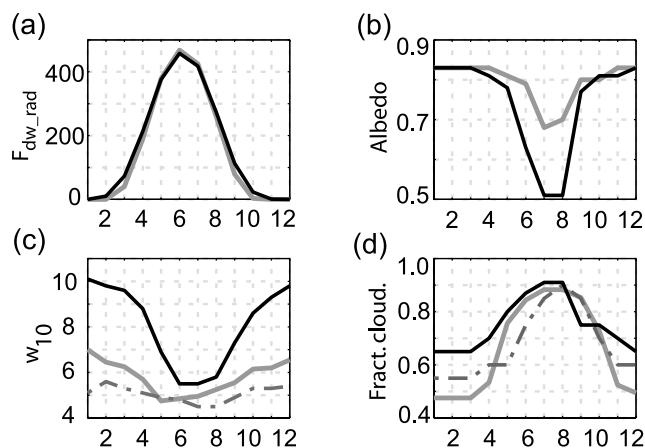
Figure 8. Atmospheric forcing parameters. Solid gray line is the Arctic Ocean model, solid black line is the Greenland Sea model, and dash-dotted gray line is shelf model. Abscissa is months. (a) Downwelling shortwave radiation, W m^{-2}. (b) Ice/snow surface albedo (based on *Maykut and Untersteiner* [1971], *Maykut* [1986], and *Lindsay* [1998]). Since ice in the Greenland Sea is less than 0.88 m, albedo is calculated from an empirical relation between albedo and ice thickness: $\alpha_{ice} = 0.44(h_{ice})^{0.28} + 0.08$ [*Maykut and Untersteiner,* 1971]. (c) Surface wind (NCEP Reanalysis from NCAR-CIRES CDC [*Lindsay,* 1998; *Polyakov et al.,* 1999]), m s^{-1}. (d) Fractional cloudiness [*Gorshkov,* 1980].

Figure 9. Hydrological forcing. Abscissa is months. (a) Bering water temperature (black dash-dotted curve), °C, and salinity (gray solid curve) [*Coachman et al.,* 1975; *Gorshkov,* 1980]. (b) Freshwater inflow (dash-dotted), ×10^5 m^3·s^{-1}, and temperature (gray solid), °C [*Gorshkov,* 1980; *Björk,* 1989]. (c) Atalntic water inflow to the Greenland Sea box (dash-dotted), Sv, and its temperature (gray solid), °C [*Swift,* 1986]. (d) Polar water inflow to the Greenland Sea box as a fraction of the total outflow from the Arctic Ocean model. Both inflows have been estimated from model sensitive runs to reproduce seasonal T and S variations in the region discussed by *Swift* [1986] and *Pawlowicz* [1995].
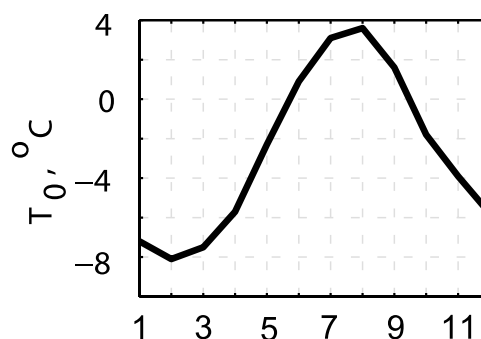

Figure 10. Prescribed surface air temperature in the Greenland Sea model.

summer and the slow deepening during the cold season which has been reported by *Lemke and Manley* [1984].

[60] The mixed layer water in the Arctic Ocean is characterized by low salinities which vary from above 34 psu north of Svalbard to below 32 psu in the Makarov Basin [*Coachman and Aagaard,* 1974; *Rudels,* 1998]. Zonally integrated salinity of the upper 10 m obtained from PHC data is plotted in Figure 11b and reveals a noticeable seasonal signal. The simulated salinity (black curve) in the mixed layer reproduces seasonality with minimum in summer and maximum by the end of the cold season. The range of the simulated seasonal salinity is in the range of observed values in the interior Arctic Ocean.

[61] Ice thickness distribution and ice production vary significantly in time and space over the Arctic Ocean [*Hibler,* 1980; *McLaren et al.,* 1994; *Wadhams,* 1994]. For the purpose of this study, we reproduced the average ice production in the central Arctic. Figure 11c presents simulated ice thickness in the Arctic model which is reasonably close to results from the model study of *Hibler* [1979]. The onset of melting is in the middle of May, and freezing starts by the middle of September.

[62] Computed and observed monthly mean SAT in the Arctic are presented in Figure 11d. The observed monthly means and their standard deviations have been estimated from the daily data for the central Arctic (86°N poleward) for the period 1948–2001. The data are NCEP reanalysis acquired from NOAA-CIRES CDC (http://www.cdc.noaa.gov). The simulated SAT has a slight cold bias in spring, being at a lower bound of the 98% confidence interval of the NCEP reanalysis data.

[63] Results from our model of the Arctic Ocean agree with output from the models of *Björk* [1989] and *Alekseev and Ryabchenko* [1996]. However, there are few quantitative discrepancies among the model results. For example, from a thermodynamical model of the sea ice – ocean system of *Alekseev and Ryabchenko* [1996], simulated mixed layer salinity ranges from ~30.8 (August) to 33.9 (June) which is too saline compared to the observations (Figure 11b). Also, the onset of freshening of the mixed layer (July) is delayed in the model of Alekseev and Ryabchenko (from our Figure 11b, observed freshening starts in May) resulting in delay of the mixed layer shallowing in summer (July).

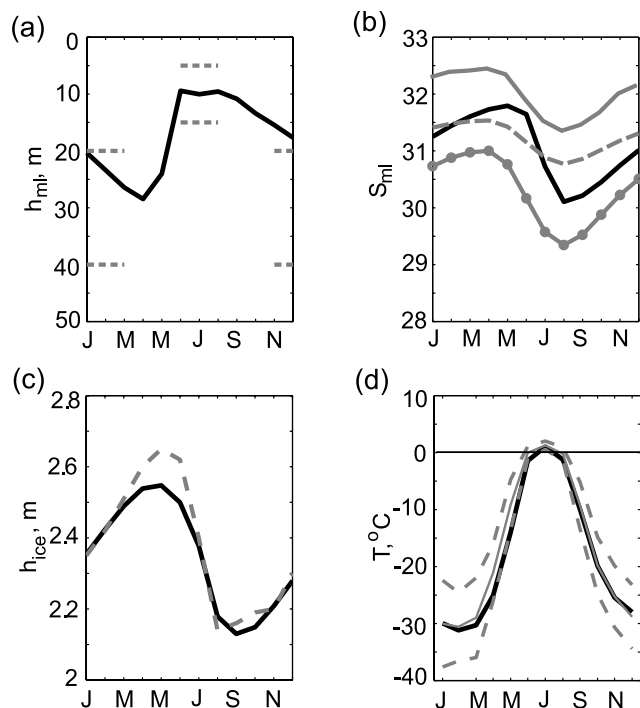[64] Mixed layer salinity calculated in the *Björk* [1989] model seems to be underestimated. It changes from ~28.8

Figure 11. Climatology from the Arctic model (black solid curves). (a) Mixed layer thickness. Dashed gray segments show the range of the mixed layer in the Eurasian and Canadian Basins for the winter and summer periods estimated from the thermohaline profiles in the *EWG* [1998] atlas. (b) Mixed layer salinity. Gray curves denote zonally averaged salinity in the upper 10 m estimated from data acquired from Polar Hydrographic Climatology [*Steele et al.*, 2001]: solid– Eurasian Basin, 82.5N; dashed– Canadian Basin, 80.5N; curve with bullets – Canadian Basin, 76.5N. (c) Ice thickness from the thermodynamic sea ice model. Gray dashed curve shows average Arctic Basin ice thickness simulated by *Hibler* [1979]. (d) SAT. Solid gray curve denotes climatology obtained from NCEP Reanalysis data (NOAA-CIRES CDC) over the period 1948–2001. Dashed gray curves denote 98% confidence interval for the NCEP Reanalysis monthly means.

terized and hence, the shelf water is isolated from solar radiation until the ice is gone.

[67] The ice model simulates 1.5 m ice on the shelf which melts by August. This agrees with the output from other models [*Hibler*, 1980; *Hibler and Walsh*, 1982; *Polyakov et al.*, 1999] that simulate ice < 2 m on the most of the Eurasian shelf and low ice concentration in August and September.

3.2.3. Greenland Sea

[68] The observed mixed layer depth in the GIN Sea varies substantially both in time and space. In summer and early autumn, the mixed layer is shallow (10–30 m) over the whole basin. Maximum thickness of the mixed layer in the GIN Sea is observed in March–May (from analysis of NODC NOAA mixed layer depth data (http://www.nodc.noaa.gov/OC5/mix.html). Due to large differences in the upper water characteristics in that region [*Swift*, 1986], the mixed layer thickness is highly variable over the GIN Sea. The maximum winter mixed layer thickness is observed in the central northern and eastern Norwegian Sea (from 400 m to 800 m), while the mixed layer in the central and western Greenland Sea is shallow (above 200 m). The model reproduces shallowing of the mixed layer in the Greenland Sea in summer (~15 m) and rapid deepening during the cold season (Figure 13a). Maximum thickness of the mixed layer (about 380 m) is simulated in April, at the end of the winter.

[69] Shown in Figure 13b is the calculated mixed layer temperature. The model output fits the observed summer temperature in the upper Greenland Sea calculated from the Polar Science Center Hydrographic Climatology (PHC). In winter, simulated mixed layer temperature reaches the freezing point and ice forms (Figure 13d). The PHC winter temperature in the upper 10 and 75 meters is also negative but much warmer than the model. Also noticeable is sudden warming of the observed temperature in April–May. The discrepancies of the simulated and observed winter water temperature indicate that in the model the underlying Atlantic Intermediate Water layer (the water at depths 250–500 m) is too cold. In this case, the mixed layer does not entrain enough heat and stays cold. However, winter temperature estimates obtained from PHC contradict monthly climatology of the Greenland Gyre (central Greenland Sea) described by *Pawlowicz* [1995]. The climatology

in September to ~30.6 in May, lower than observed values (Figure 11b). Björk's mixed layer depth variability is similar to our model shown in Figure 11a.

3.2.2. Shelf

[65] Seasonal variability is well pronounced in the Arctic shelf seas (compare gray curves in Figures 12a and 12b of averages for the East-Siberian, Laptev, and Kara Seas). The shelf model reproduces the seasonal signal in shelf water salinity (Figure 12a) and temperature (Figure 12b). The model amplitude of the salinity variations is smaller, and the computed annual mean salinity is lower, than in observations.

[66] Shelf water temperature stays near the freezing point during the winter and rapidly warms to -0.2°C after the ice melts (Figure 12c). The observed seasonal cycle of the water temperature in the upper 50 m layer on the shelf is smoother than simulated. The onset of warming is in May–June when river runoff increases and shelf water gains energy through leads. In the model, leads are not parame-
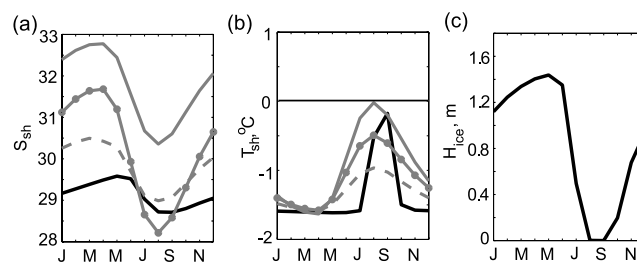

Figure 12. Climatology from the shelf model. (a) Shelf water salinity. Gray curves are mean salinities integrated in the upper 50 m from data acquired from Polar Hydrographic Climatology [*Steele et al.*, 2001]: solid – Kara Sea; curve with bullets – Laptev Sea; dashed – East-Siberian Sea. (b) Similar to Figure 12a, but for the shelf water temperature. (c) Ice thickness from thermodynamic sea ice model.
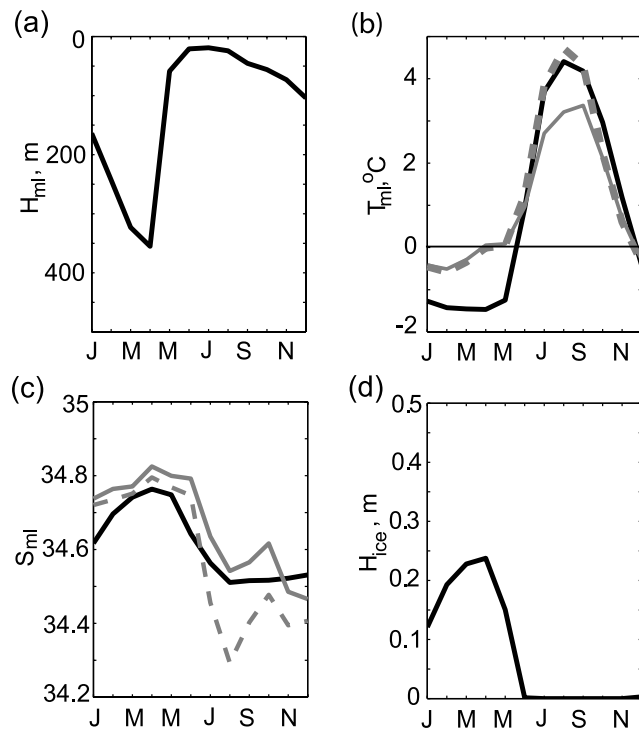
Figure 13. Climatology from the Greenland Sea model. (a) Mixed layer thickness. (b) Mixed layer temperature. Gray curves show mean temperatures in the central Greenland Sea estimated from data acquired from PHC: dashed curve – in the upper 10 m; solid curve – in the upper 75 m. Note that the winter temperature is the same for 10 and 75 m indicating a homogeneous mixed layer at this time of year. In summer, the temperature differs due to seasonal shallowing of the mixed layer. (c) Similar to Figure 13b, but for the mixed layer salinity. (d) Ice thickness from the thermodynamic sea ice model.

has been created based on historical archives of hydrographic stations and observations from cruises. According to *Pawlowicz* [1995], water temperature of the upper Greenland Gyre "... presumably remains near the freezing point from November to February ... In March the midgyre surface warms to about −1.4°C through mixing with deeper and warmer waters ... but does not warm much more until May ...". The simulated winter temperature presented in Figure 13b is similar to the midgyre temperature at 160–200 m shown by *Pawlowicz* [1995, Figure 4b]. From the figure in *Pawlowicz* [1995] it follows that the winter temperature at this depth is colder than −1°C, similar to our simulated winter temperature and not the PHC results.

[70] The general features of the annual, upper layer salinity cycle are well reproduced in the model (Figure 13c). The salinity increases during winter from entrainment of more saline underlying water and from salt rejection. With the onset of ice melt, in late May – early June, the mixed layer freshens and stays diluted until the start of thermohaline convection and ice freezing. There are only minor discrepancies between the model and the observations. The behavior of the observed salinity in the upper Greenland Sea is more complex (gray curves in Figure 13c) than in the model. In particular, there are small peaks

imposed on the seasonal variability described earlier, perhaps due to precipitation which is not taken into account in the analyzed model. Also advection of fresh and salt water into the Greenland Sea is not as regular and stationary as in the model (Figures 9c and 9d).

4. Discussion

[71] The Arctic Ocean model exhibits the best correspondence to the observations compared to the other sub-models because the dynamics and thermohaline changes of the mixed layer are mainly controlled by the ice freeze/melt cycle. This relationship is well reproduced in the model. In winter, intense ice formation leads to the mixed layer salinification (equation (8)). The water column becomes less stable (g' decreases). Weak water column stability and strong and negative buoyancy flux at the surface (equation (7)) promote a high entrainment velocity (equation (6)) and deepening of the mixed layer (Figure 11a). Also, the simulated shelf water has higher salinity in winter (Figure 12a) due to lower river runoff (Figure 9b) and higher ice production (Figure 12c). That makes the salinity of the shelf water inflow to the mixed layer (S_{sh_ml}) higher and, hence, reduces the positive contribution to the buoyancy flux (equation (7)) promoting mixed layer deepening. In summer, intense ice melt, first in the shelf box and then in the Arctic domain, freshens the upper layer, increases the water column stability, and stops entrainment. The mixed layer then thins (Figure 11a).

[72] Underestimated SAT in spring may result from the absence of meridional latent heat transport in the atmospheric model. As mentioned earlier, only sensible heat transport is considered in the model (equation (25)). In the real Arctic climate system, the latent heat transport plays a significant role. However, the contribution of these two transports to the meridional heat transport is different during the year [*Jackson and Broccoli*, 2003]. It might be that in spring the latent heat transport to the Arctic is essential and neglecting it in the atmospheric model has led to the cold bias.

[73] The shelf model reproduces seasonality, although the shelf water salinity is lower than the PHC data (Figure 12a). Note that spatially averaged salinity decreases eastward as the distance from the North Atlantic increases. The salinity in the East-Siberian Sea is close to the simulated shelf salinity. Hence, the most likely reason for the negative salinity bias in the box model is an underestimation of the advection of Atlantic water. Another reason for the fresh bias may be the lack of dynamics in the sea ice model.

[74] A sensitivity analysis of the model parameters has been conducted (for details, see *Dukhovskoy* [2003]). The key parameters controlling the annual cycle in the Arctic Ocean and shelf models are the mixed layer outflow to the shelf (Q_{mao}), and the coefficient of heat advection (χ); in the Greenland Sea model the key parameters are the ratio of the Polar Water (Q_{PW}) and Atlantic Water (Q_{AtW}) inflows (equations (26) and (27)) and the proportionality coefficient κ which parameterizes dissipation of free convection in the formula for entrainment velocity (equation (6)).

[75] In the shelf model ($Q_{mao} = Q_{sh}$) Q_{mao} determines the amount of fresh water advected to the Arctic Ocean model. The sensitivity experiments have been fulfilled for different

values of Q_{mao} from 0.1 to 2 Sv. Low values lead to quick salinization of the upper Arctic Ocean, unrealistically deep mixed layer and unstable solutions. Stable and realistic behaviors of the Arctic Ocean model have been obtained for Q_{mao} = 1.1 to 1.8 Sv.

[76] The coefficient of heat advection has been tested for values ranging from 0.5 to 4 W m^{-2} °K^{-1}. The sensitivity analysis has revealed that the lower values of χ lead to a colder Arctic as expected. The variability of SAT induced by different χ is larger in the cold season. However, the summer amplitude of SAT is small because the Arctic gains substantial solar radiation and heat advection is not a primary source of energy. The case $\chi = 0.5$ W $\cdot$ m^{-2} $\cdot$°K^{-1} results in an unrealistically cold Arctic. The opposite case $\chi = 4.0$ W $\cdot$ m^{-2} $\cdot$ °K^{-1} leads to a very warm Arctic. When $\chi = 1.8$ to 2. W $\cdot$ m^{-2} $\cdot$ °K^{-1} the model reproduces the observed SAT.

[77] The dynamics of the mixed layer in the Greenland Sea model are very sensitive to the temperature and salinity of the upper and underlying layers. Thermohaline characteristics of the upper layer in the model are determined by the ratio of the inflow of Polar Water to Atlantic Water. A number of "tune-up" experiments has been run to adjust the unknown values of Q_{PW} and Q_{AtW}. If the amount of Polar Water incoming to the Greenland Sea model is too high, the convection in winter is sluggish. In the opposite case, when the Atlantic Water inflow is too high, the convection is fast and reaches the bottom of the model water column in a few time steps. In particular, the annual mean ratio $Q_{PW}/Q_{AtW} \approx 3.7 \times 10^{-2}$ leads to low water column stability in the Greenland Sea, with highly possible deep convection. For $Q_{PW}/Q_{AtW} \approx 8.0 \times 10^{-2}$, there is strong freshening of the upper Greenland Sea and deep convection ceases. In these experiments the ratio is approximately 6×10^{-2}.

[78] Another free parameter that determines upper layer dynamics is κ (equation (6)). As discussed earlier, this coefficient parameterizes dissipation of the convectively produced turbulence. Different approaches to parameterize κ have been tested. The major finding of this sensitivity analysis is that, although it works well for the Arctic Ocean, constant κ results in false dynamics of the mixed layer in the Greenland Sea. Having κ a function of the water column stability (equation (30)) gives more realistic behavior of the upper layer of the Greenland Sea model.

5. Summary

[79] An idealized multibox model of the Arctic Ocean and GIN Sea has been developed, calibrated and validated. The model is used to investigate possible mechanisms of decadal climate variability in the Arctic based on existing concepts of Arctic decadal oscillations. The model presented in this paper realistically describes the major oceanographic and atmospheric characteristics in the Arctic and Greenland Sea over the annual cycle and could be used for investigation of interannual and decadal variability of Arctic climate.

[80] From the validation experiment, we found that the behavior of the Arctic module is in good agreement with observations for the whole annual cycle and has similarities to the dynamics reproduced in the integral models of Björk

[1989] and *Alekseev and Ryabchenko* [1996]. Compared with observations, our model shows better performance for the mixed layer salinity (Figure 11b). The atmospheric model simulates Arctic SAT reasonably close to the observations with a slight negative bias in spring.

[81] The shelf model reproduces seasonality of the oceanic characteristics similar to the observations (Figure 12). The shelf water salinity is lower than the spatially averaged salinity in the upper 50 m of the Laptev, Kara, and East-Siberian seas. Based on the good performance of the Arctic Ocean model, it is believed that the small salinity bias in the shelf model is admissible because it has minimal impact on the solution in the interior domain.

[82] The Greenland Sea model simulates seasonal variability in the ice-ocean component (recall that in the validation experiment, the model was forced with daily climatological mean SAT) in general agreement with observations (Figure 13). Winter mixed layer temperature in the model (Figure 13b) is colder than water temperature from PHC integrated over 10 and 75 meters but is in good agreement with *Pawlowicz* [1995]. Salinity calculated in the model is similar to the observed values (Figure 13c) which is evidence that the salt balance is well reproduced in the simulated system.

Notation

A_{AO}	area of the Arctic Ocean model domain (0.61 × 10^{13} m^2).
A_{GS}	area of the Greenland Sea model domain (0.135 × 10^{12} m^2).
A_{sh}	area of the shelf region (0.41 × 10^{13} m^2).
B_{fl}	buoyancy flux.
C_p	air specific heat (1012 J kg^{-1} °K^{-1}).
C_{wp}	water specific heat (4184.4 J m^{-2}·sec^{-1}).
D_z	coefficient of vertical eddy diffusivity (1. × 10^{-6} m^2 s^{-1}).
F_{adv}	meridional sensible heat advection to the Arctic atmospheric box model.
F_{tot}	surface heat flux.
F_{tot_a}	energy balance in the atmospheric box model.
$\bar{F}_w$	water heat flux to the ice bottom.
g	gravitational acceleration.
g'	reduced gravity.
H_{atm}	height of the atmospheric box (8 km).
H_{AtW}	thickness of the Atlantic Water flowing into the Greenland Sea model.
H_h	total thickness of the mixed layer and halocline.
h_{Ekm}	Ekman depth scale.
h_{Ob}	Monin-Obukhov depth scale.
h_{ice}	ice thickness.
h_{ml}	mixed layer depth.
H_{PW}	thickness of the Polar Water flowing into the Greenland Sea model.
h_{sh}	depth of the shelf box.
h_{shw}	depth of the shelf box measured from the base of the ice.
h_w	mixed layer thickness without ice draft.
m_0	entrainment proportionality coefficient for dissipation of forced convection.
Pr_{i_ao}	ice production in the Arctic Ocean model.
Pr_{i_GS}	ice production in the Greenland Sea model.

Pr_{i_sh} ice production in the shelf model.

Q_{AtW} Atlantic water inflow to the Greenland Sea.

Q_{atl_sh} Atlantic water inflow to the shelf.

Q_{Ber} the Bering Strait inflow to the Arctic Ocean.

Q_f river runoff.

Q_{g_atl} total Arctic Ocean outflow to the North Atlantic.

Q_{gML_atl} Arctic Ocean outflow to the North Atlantic from mixed layer.

Q_{GSDW} Greenland Sea Deep Water inflow to the Greenland Sea.

Q_{ice} ice export from the Arctic Ocean and shelf models.

Q_{lAIW} lower Arctic Intermediate Water inflow to the Greenland Sea.

Q_{mao} inflow to the shelf box from the Arctic mixed layer (1.1 Sv).

Q_{mlt_GS} volume of ice melted in the Greenland Sea model.

Q_{NSDW} Norwegian Sea Deep Water inflow to the Greenland Sea.

$Q_{(P-E)}$ net precipitation flux.

Q_{PW} Polar Water inflow to the Greenland Sea.

Q_{sh} total shelf outflow to the interior Arctic Ocean.

$q_{sh}(z)$ shelf outflow at a given depth z.

Q_{sh_ml} shelf outflow to the interior Arctic Ocean mixed layer.

Q_{uAIW} upper Arctic Intermediate Water inflow to the Greenland Sea.

q_0 shelf outflow at salinity equal to shelf water salinity.

S_{atl} salinity of the Atlantic layer in the Arctic Ocean model.

S_{ml} mixed layer salinity.

S_{PW} Polar Water salinity.

S_{sh} salinity in the shelf box model.

$\bar{S}_{sh\_ml}$ integrated salinity of the shelf outflow into the mixed layer.

$S_{sh\_out}(z)$ salinity of the shelf outflow at a given depth z.

S_{xx} maximum salinity where shelf outflow function, q_{sh}, becomes zero.

T_0 surface air temperature.

T_{PW} Polar Water temperature.

T_{atl} temperature of the Atlantic water.

T_{ml} mixed layer temperature.

T_{sh} water temperature in the shelf box model.

u_* friction velocity.

w_a vertical velocity.

w_e entrainment velocity.

α coefficient of heat expansion.

β coefficient of salt contraction.

ε ratio of sea ice density to sea water density (0.9).

κ entrainment proportionality coefficient for dissipation of free convection.

λ_{out} number of outlets in Arctic Ocean model for total outflow to the North Atlantic (1.5).

μ_{Ber} coefficient for Bering water inflow to the Arctic.

ξ fraction of the rejected salt consumed for the shelf water salinity increase.

ρ_{ao} the Arctic Ocean density at a given depth level (z).

ρ_{ml} mixed layer density.

$\rho_{sh\_out}(z)$ density of the shelf outflow at a given depth z.

ϕ total outflow of salt from the shelf box model.

χ coefficient of heat advection.

References

Aagaard, K., and E. C. Carmack (1989), The role of sea ice and other freshwater in the Arctic circulation, *J. Geophys. Res.*, *94*, 14,485–14,498.

Aagaard, K., and E. C. Carmack (1994), The Arctic and climate: A perspective, in *Polar Oceans and Their Role in Shaping the Global Environment, Geophys. Monogr. Ser.*, edited by O. M. Johannessen et al., pp. 4–20, AGU, Washington, D. C.

Aagaard, K., L. K. Coachman, and E. C. Carmack (1981), On the halocline of the Arctic Ocean, *Deep Sea Res.*, *28*, 529–545.

Alekseev, G. V., and V. A. Ryabchenko (1996), Reconstruction of the seasonal variability of the sea ice-ocean system in the Arctic Basin (in Russian), *Proc. Acad. Sci. Phys. Atmos. Ocean*, *32*, 581–590.

Alekseev, G. V., V. V. Ivanov, and A. A. Korablev (1994), Interannual variability of the thermohaline structure in the convective gyre of the Greenland Sea, in *Polar Oceans and Their Role in Shaping the Global Environment, Geophys. Monogr. Ser.*, edited by O. M. Johannessen et al., pp. 485–496, AGU, Washington, D. C.

Björk, G. (1989), A one-dimensional time-dependent model for the vertical stratification of the upper Arctic Ocean, *J. Phys. Oceanogr.*, *19*, 52–67.

Chapman, D. C. (1997), A note on isolated convection in a rotating two-layer fluid, *J. Fluid Mech.*, *348*, 319–325.

Chatfield, C. (1996), *The Analysis of Time Series: An Introduction*, 283 pp., CRC Press, Boca Raton, Fla.

Claussen, M., et al. (2002), Earth system models of intermediate complexity: Closing the gap in the spectrum of climate system models, *Clim. Dyn.*, *18*, 579–586.

Coachman, L. K., and K. Aagaard (1974), Physical oceanography of the arctic and sub-arctic seas, in *Marine Geology and Oceanography of the Arctic Ocean*, edited by Y. Herman, pp. 1–72, Springer, New York.

Coachman, L. K., K. Aagaard, and R. B. Tripp (1975), *Bering Strait: The Regional Physical Oceanography*, 175 pp., Univ. of Wash. Press, Seattle.

Curry, J. A., and A. H. Lynch (2002), Comparing Arctic regional climate models, *Eos Trans. AGU*, *83*(9), 87.

Cushman-Roisin, B. (1994), *Introduction to Geophysical Fluid Dynamics*, 290 pp., Prentice-Hall, Upper Saddle River, N.J.

Doronin, Y. P. (1997), Sea ice freezing and melting, in *Sea Ice (in Russian)*, edited by N. P. Muravieva, pp. 68–106, Gidrometeoizdat, St. Petersburg.

Dukhovskoy, D. S. (2003), Decadal variability in the Arctic Ocean - Greenland-Iceland-Norwegian Seas ice-ocean-atmosphere climate system, Ph.D. thesis, Univ. of Alaska Fairbanks, Fairbanks.

Dukhovskoy, D., M. Johnson, and A. Proshutinsky (2006), Arctic decadal variability from an idealized atmosphere-ice-ocean model: 2. Simulation of decadal oscillations, *J. Geophys. Res.*, *111*, C06029, doi:10.1029/2004JC002820.

Environmental Working Group (EWG) (1998), *Joint U.S. Russian Atlas of the Arctic Ocean for the Winter/Summer Period* [CD-ROM], Natl. Snow and Ice Data Cent., Boulder, Colo.

Flato, G. M., G. J. Boer, W. G. Lee, N. A. McFarlane, D. Ramsden, M. C. Reader, and A. J. Weaver (2000), The Canadian Centre for Climate Modelling and Analysis global coupled model and its climate, *Clim. Dyn.*, *16*, 451–467.

Fletcher, C. A. J. (1988), *Computational Techniques for Fluid Dynamics*, vol. 1, *Fundamental and General Techniques*, 457 pp., Springer, New York.

Goosse, H., F. Selten, R. Haarsma, and J. Opsteegh (2003), Large sea-ice volume anomalies simulated in a coupled climate model, *Clim. Dyn.*, *20*, 523–536, doi:10.1007/s00382-002-0290-4.

Gordon, C., C. Cooper, C. A. Senior, H. T. Banks, J. M. Gregory, C. Johns, J. F. B. Mitchell, and R. A. Wood (2000), The simulation of SST, sea ice extents and ocean heat transports in a version of the Hadley Centre coupled model without flux adjustments, *Clim. Dyn.*, *16*, 147–168.

Gordon, H. B., and S. P. O'Farrell (1997), Transient climate change in the CSIRO coupled model with dynamic sea ice, *Mon. Weather Rev.*, 125, 875–907.

Gorshkov, S. G. (1980), Atlas of Oceans: The Arctic Ocean, Minist. of Def. of the USSR, Moscow.

Häkkinen, S. (1995), Simulated interannual variability of the Greenland Sea deep water formation and its connection to surface forcing, *J. Geophys. Res.*, 100, 4761–4770.

Häkkinen, S. (2000), Decadal air-sea interaction in the North Atlantic based on observations and modeling results, *J. Clim.*, 13, 1195–1219.

Häkkinen, S., and D. J. Cavalieri (1989), A study of oceanic surface heat fluxes in the Greenland, Norwegian, and Barents Seas, *J. Geophys. Res.*, 94, 6145–6157.

Häkkinen, S., and G. L. Mellor (1990), One hundred years of Arctic ice cover variations as simulated by a one-dimensional coupled ice-ocean model, *J. Geophys. Res.*, 95, 15,959–15,969.

Henderson-Sellers, A., and K. McGuffie (1987), *A Climate Modelling Primer*, 217 pp., John Wiley, Hoboken, N. J.

Hibler, W. D., III (1979), A dynamic thermodynamic sea ice model, *J. Phys. Oceanogr.*, 9, 815–846.

Hibler, W. D., III (1980), Modeling a variable thickness sea ice cover, *Mon. Weather Rev.*, 108, 1943–1973.

Hibler, W. D., III, and J. E. Walsh (1982), On modeling seasonal and interannual fluctuations of the Arctic sea ice, *J. Phys. Oceanogr.*, 12, 1514–1523.

Houssais, M.-N. (1987), Testing a coupled ice-mixed-layer model under subarctic conditions, *J. Phys. Oceanogr.*, 18, 196–210.

Iqbal, M. (1983), *An Introduction to Solar Radiation*, 390 pp., Elsevier, New York.

Jackson, C. S., and A. J. Broccoli (2003), Orbital forcing of Arctic climate: Mechanisms of climate response and implications for continental glaciation, *Clim. Dyn.*, 21, 539–557, doi:10.1007/s00382-003-0351-3.

Jennrich, R. I. (1995), *An Introduction to Computational Statistics: Regression Analysis*, 364 pp., Prentice-Hall, Upper Saddle River, N. J.

Johannessen, O. M. (1986), Brief overview of the physical oceanography, in *The Nordic Seas*, edited by B. G. Hurdle, pp. 103–127, Springer, New York.

Jonsson, S. (1991), Seasonal and interannual variability of wind stress curl over the Nordic Seas, *J. Geophys. Res.*, 96, 2649–2659.

Kato, H., and O. M. Phillips (1969), On the penetration of a turbulent layer into a stratified fluid, *J. Fluid Mech.*, 37, 643–655.

Killworth, P. D. (1979), On "chimney" formation in the ocean, *J. Phys. Oceanogr.*, 9, 531–554.

Killworth, P. D., and J. M. Smith (1984), A one-and-half dimensional model for the Arctic halocline, *Deep Sea Res.*, 31, 271–293.

Kreyszig, E. (1999), *Advanced Engineering Mathematics*, 1156 pp., John Willey, Hoboken, N. J.

Lemke, P. (1987), A coupled one-dimensional sea ice-ocean model, *J. Geophys. Res.*, 92, 13,164–13,172.

Lemke, P., and T. O. Manley (1984), The seasonal variation of the mixed layer and the pycnocline under the polar sea ice, *J. Geophys. Res.*, 89, 6494–6504.

Lindsay, R. W. (1998), Temporal variability of the energy balance of thick Arctic pack ice, *J. Clim.*, 11, 313–333.

Makshtas, A. P. (1991), *The Heat Budget of Arctic Ice in the Winter*, 77 pp., Int. Glaciol. Soc., Cambridge.

Manabe, S., and R. J. Stouffer (1996), Low-frequency variability of surface air temperature in a 1000-year integration of a coupled atmosphere-ocean-land surface model, *J. Clim.*, 9, 376–393.

Marotzke, J., and P. H. Stone (1995), Atmospheric transports, the thermohaline circulation, and flux adjustments in a simple coupled model, *J. Phys. Oceanogr.*, 25, 1350–1364.

Maykut, G. A. (1986), The surface heat and mass balance, in *The Geophysics of Sea Ice*, edited by N. Untersteiner, pp. 395–463, Springer, New York.

Maykut, G. A., and N. Untersteiner (1969), Numerical prediction of the thermodynamic response of Arctic sea ice to environmental changes, 173 pp., The Rand Corp., Santa Monica, Calif.

Maykut, G. A., and N. Untersteiner (1971), Some results from a time-dependent thermodynamic model of sea ice, *J. Geophys. Res.*, 76, 1550–1575.

McLaren, A. S., R. H. Bourke, J. E. Walsh, and R. L. Weaver (1994), Variability in sea-ice thickness over the North Pole from 1958 to 1992, in *Polar Oceans and Their Role in Shaping the Global Environment*, *Geophys. Monogr. Ser.*, edited by O. M. Johannessen et al., pp. 363–371, AGU, Washington, D. C.

Miropolsky, Y. Z., B. N. Filyushkin, and P. P. Chernyshkov (1969), On the parametric description of temperature profiles in the active ocean layer, *Oceanology*, 10, 892–897.

Mysak, L. A., K. M. Wright, J. Sedlacek, and M. Eby (2005), Simulation of sea ice and ocean variability in the Arctic during 1955–2002 with an intermediate complexity model, *Atmos. Ocean*, 43, 101–118.

Niiler, P. P., and E. B. Kraus (1977), One-dimensional models of the upper ocean, in *Modelling and Prediction of the Upper Layers of the Ocean*, edited by E. B. Kraus, chap. 10, pp. 143–172, Elsevier, New York.

North, G. R. (1975), Theory of energy-balance climate models, *J. Atmos. Sci.*, 32, 2033–2043.

Pawlowicz, R. (1995), A note on seasonal cycles of temperature and salinity in the upper waters of the Greenland Sea Gyre from historical data, *J. Geophys. Res.*, 100, 4715–4726.

Polyakov, I. V., A. Y. Proshutinsky, and M. A. Johnson (1999), Seasonal cycles in two regimes of Arctic climate, *J. Geophys. Res.*, 104, 25,761–25,788.

Proshutinsky, A., R. H. Bourke, and F. A. McLaughlin (2002), The role of the Beaufort Gyre in Arctic climate variability: Seasonal to decadal climate scales, *Geophys. Res. Lett.*, 29(23), 2100, doi:10.1029/2002GL015847.

Robitaille, D. Y., L. A. Mysak, and M. S. Darby (1995), A box model study of the Greenland Sea, Norwegian Sea and Arctic Ocean, *Clim. Dyn.*, 11, 51–70.

Rudels, B. (1998), Aspects of Arctic oceanography, in *Physics of Ice-Covered Seas: Lecture Notes From a Summer School in Savonlinna, Finland 6–17 June 1994*, edited by M. Lepparanta, pp. 517–569, Helsinki Univ. Print. House, Helsinki.

Rudels, B., H. J. Friedrich, D. Hainbucher, and G. Lohman (1999), On the parameterization of oceanic sensible heat loss to the atmosphere and to ice in an ice-covered mixed layer in winter, *Deep Sea Res., Part II*, 46, 1385–1425.

Saltzman, B. (1985), Paleoclimatic modeling, in *Paleoclimatic Analysis and Modeling*, edited by A. D. Hecht, pp. 341–396, John Wiley, Hoboken, N. J.

Scott, J. R., J. Marotzke, and P. H. Stone (1999), Interhemispheric thermohaline circulation in a coupled box model, *J. Phys. Oceanogr.*, 29, 351–365.

Shindell, D. (2003), Whither Arctic climate?, *Science*, 299, 215–216.

Steele, M., D. Thomas, D. Rothrock, and S. Martin (1996), A simple model study of the Arctic Ocean freshwater balance, 1979–1985, *J. Geophys. Res.*, 101, 20,833–20,848.

Steele, M., R. Morley, and W. Ermold (2001), PHC: A global ocean hydrography with a high quality Arctic Ocean, *J. Clim.*, 14, 2079–2087.

Stigebrandt, A. (1981), A model for the thickness and salinity of the upper layer in the Arctic Ocean and the relationship between ice thickness and some external parameters, *J. Phys. Oceanogr.*, 11, 1407–1422.

Stigebrandt, A. (1985), A model for the seasonal pycnocline in rotating systems with application to the Baltic proper, *J. Phys. Oceanogr.*, 15, 1392–1404.

Stone, P. H., and M.-S. Yao (1990), Development of a two-dimensional zonally averaged statistical-dynamical model. Part III: The parameterization of the eddy fluxes of heat and moisture, *J. Clim.*, 3, 726–740.

Swift, J. H. (1986), The Arctic waters, in *The Nordic Seas*, edited by B. G. Hurdle, pp. 129–153, Springer, New York.

Swift, J. H., and K. Aagaard (1981), Seasonal transition and water mass formation in the Iceland and Greenland seas, *Deep Sea Res., Part A*, 28, 1107–1129.

Swift, J. H., E. P. Jones, K. Aagaard, E. C. Carmack, M. Hingston, R. W. Macdonald, F. A. McLaughlin, and R. G. Perkin (1997), Waters of the Makarov and Canada basins, *Deep Sea Res.*, 44, 1503–1529.

Thorndike, A. S., and R. Colony (1982), Sea ice motion in response to geostrophic winds, *J. Geophys. Res.*, 87, 5845–5852.

Turner, J. S. (1973), *Buoyancy Effects in Fluids*, 367 pp., Cambridge Univ. Press, New York.

Visbeck, M., J. Fischer, and F. Schott (1995), Preconditioning the Greenland Sea for deep convection: Ice formation and ice drift, *J. Geophys. Res.*, 100, 18,489–18,502.

Wadhams, P. (1994), Sea ice thickness changes and their relation to climate, in *Polar Oceans and Their Role in Shaping the Global Environment*, *Geophys. Monogr. Ser.*, edited by O. M. Johannessen et al., pp. 337–361, AGU, Washington, D. C.

Walin, G. (1993), On the formation of ice on deep weakly stratified water, *Tellus, Ser. A*, 45, 143–157.

Wallace, J. M., and P. V. Hobbs (1977), *Atmospheric Science: An Introductory Survey*, 467 pp., Elsevier, New York.

Wang, Z., and L. A. Mysak (2000), A simple coupled atmosphere-ocean-sea ice-land surface model for climate and paleoclimate studies, *J. Clim.*, 13, 1150–1172.

_____

D. Dukhovskoy, Center for Ocean-Atmospheric Prediction Studies, Florida State University, Tallahassee, FL 32306, USA. (ddmitry@coaps.fsu.edu)

M. Johnson, Institute of Marine Science, University of Alaska Fairbanks, Fairbanks AK 99775, USA.

A. Proshutinsky, Physical Oceanography Department, Woods Hole Oceanographic Institution, Woods Hole, MA 02543 USA.